RSC Sustainability

ROYAL SOCIETY OF CHEMISTRY

CRITICAL REVIEW

View Article Online
View Journal | View Issue

Cite this: *RSC Sustainability*, 2025, **3**, 3628

Recent advances in MOFs, MOF-derived materials and their composites as electrocatalysts for hydrogen production

E. S. Sowbakkiyavathi,[ad] Preethi Dhandapani,[b] Senthilkumar Ramasamy,[c] Ju Hyun Oh,[d] Insik In,[d] Seung Jun Lee*[d] and A. Subramania*[bd]

Climate change, global warming, and other adverse environmental impacts are largely driven by carbon dioxide (CO_2) emissions. One promising pathway to mitigate these issues is the growing eco-friendly hydrogen production technologies. Hydrogen, as a clean energy carrier, has the potential to transition industries toward decarbonization. Amongst the numerous hydrogen production approaches, water splitting *via* electrocatalysis presents a sustainable route. However, achieving huge productivity in the hydrogen evolution reaction (HER) requires advanced catalytic agents with enhanced active sites, huge porosity, and robust adaptability. Recently, materials based on metal–organic frameworks (MOFs) have received more consideration in electrocatalysis for environmental remediation and energy. The metal component of MOFs typically consists of metal ions (often transition metals) or metal clusters. These metal ions act as the nodes in the framework, coordinating with the organic ligands. The choice of metal determines the chemical properties, stability, and reactivity of the MOF. Numerous MOF-based materials were effectively established for the applications of the hydrogen evolution process. To produce hydrogen, this review article examines various MOF-related electrocatalysts, which include MOF-derived metals, metal oxides, metal phosphides, metal nitrides, metal chalcogenides, dichalcogenides, and their composites. Furthermore, the pros and cons of various MOF-based materials as water-splitting catalysts are discussed. Lastly, the present challenges and future prospects of these materials as electrocatalysts are also discussed.

Received 19th March 2025
Accepted 6th June 2025

DOI: 10.1039/d5su00199d

rsc.li/rscsus

Sustainability spotlight

Metal–organic framework-based electrocatalysts can be used in electrolyzers to produce hydrogen from water, offering a promising route for sustainable hydrogen production due to their individual properties like high specific area, high porosity, wide open structure, and tunability. Recently, metal–organic frameworks (MOFs) demonstrated high efficiency in the hydrogen evolution reaction (HER), with some reports showing overpotentials as low as 10 mV.

1. Introduction

Green and renewable energy must be produced to replace non-renewable resources like fossil fuels due to the world's growing energy needs and environmental concerns. When traditional fossil fuels are used, a considerable quantity of CO_2 is produced, which has led to concerns about world ecological challenges, especially global warming, ozone layer destruction, *etc.*[1–4] To explore novel, environmentally friendly, sustainable, and efficient energy sources, hydrogen is the best substitute source for the twenty-first century because of its many sources, high combustion calorific value, pollution-free nature, and other attributes. However, hydrogen sources do not exist in nature.[5]

Consequently, several techniques, such as the reformation of steam methane, the combustion of coal, and the splitting of water, were investigated to produce hydrogen for industrial purposes.[6,7] Though coal gasification and steam methane reforming can produce a significantly larger amount of hydrogen than water electrolysis, further issues, including CO_2 emissions and precursors made from fossil fuels, must be considered. Thus, the electrocatalytic water-splitting method of producing hydrogen is highly regarded. It is much more affordable, environmentally friendly, and more practical than

[a]*Department of Physics, Sathyabama Institute of Science and Technology, Chennai 600 119, India*
[b]*Electro-Materials Research Laboratory, Centre for Nanoscience and Technology, Pondicherry University, Puducherry 605 014, India. E-mail: a.subramania@gmail.com*
[c]*Centre of Excellence in Advanced Materials and Green Technologies, Amrita School of Engineering, Amrita Vishwa Vidyapeetham University, Coimbatore-641112, India*
[d]*Department of IT-Energy Convergence, Korea National University of Transportation, Chungju 27469, Republic of Korea. E-mail: sjlee@ut.ac.kr*

other approaches because it employs abundant water as the base material and limitless solar energy as the driving force.[7–9]

The procedure for water splitting in an electrolytic cell comprises two essential half-reactions: the cathodic hydrogen evolution reaction (HER) and the oxygen evolution reaction (OER). In essence, compared to the HER, the OER process needs a high overpotential to achieve the necessary current density. As a prerequisite for the thermodynamically uphill process to occur in the electrolyzer, water splitting involves a thermodynamic Gibbs free energy (DG) of about 237.2 kJ mol^{-1}, which is comparable to a standard potential (DE) of 1.23 V *versus* the reversible hydrogen electrode (RHE). Homogeneous and heterogeneous catalysts are the two different kinds of water-splitting catalysts; of these, semiconductor catalysts, as heterogeneous catalysts, have attracted a lot of interest owing to their robust anti-toxicity, huge thermal endurance, and adaptable catalytic characteristics.[10–12]

Omar Yaghi and his colleagues introduced the concept of metal–organic frameworks (MOFs) in the 1990s by demonstrating that metal ions and organic linkers could self-assemble into highly porous crystalline structures. Since then, MOFs have attracted significant attention as electrocatalysts for water splitting due to their high surface area, tunable porosity, and diverse chemical compositions. Initially developed for gas storage and separation applications, MOFs have since been adapted for catalytic purposes, including electrocatalytic water splitting, owing to their ability to be engineered with specific active sites and tailored pore architectures. Crystalline permeable polymers composed of organic intermediates and metal ions, which are identified as metal–organic frameworks (MOFs), were found to be a promising candidate in numerous fields, because of their characteristics like excellent specific area, wide open structures, high porosity, tunability, *etc.*[13]

The following are the unique properties of MOFs as an ideal candidate for application in electrocatalytic reactions. Because of their high porosity, MOFs have a wide surface area and make it easier for ions and electrons to move freely during electrochemical reactions.[14,15] During synthesis, MOF characteristics like pore size, metal sites, and ligand functionalization can be adjusted to optimize them for particular electrocatalytic reactions. MOFs may be more effective than conventional catalysts due to their enormous surface area, which frequently exceeds 7000 m^2 g^{-1}, and offer more active sites for electrochemical processes. During electrochemical reactions, the metal centers in MOFs can experience reversible coordination changes that increase their catalytic activity. MOFs with conductive metal centers or functionalized linkers can help enhance charge transfer during electrocatalytic reactions.[16,17] Hybridization with conductive materials like graphene or carbon nanotubes can improve the overall conductivity of MOFs, which is critical for efficient electrocatalysts. MOFs have a well-organized donor–acceptor interface that allows for efficient electron–hole separation and improved porosity, making them excellent candidates for use in electrocatalysis.[18] However, in their pristine form, the majority of them have limited stability in water, weak photocatalytic activity, and chemical instability. These constraints make it difficult to employ them for environmental remediation. Nonetheless, MOFs have a special feature that allows for easy tuning of their chemical compositions, allowing for the modification of both their structural and chemical characteristics to improve performance. Numerous changes, such as manufacturing heterostructures and defect engineering of heterojunctions, have been recently documented. Researchers can improve the reliability, conductivity, and reactivity of MOFs by altering the metal centers or organic ligands. By integrating MOFs with conductive substances like graphene or carbon nanotubes, their electrical conductivity and stability can be increased, increasing their usefulness for electrocatalytic processes.[19,20] By adding dopants like sulfur or nitrogen to the structure of MOFs, their stability and electrochemical characteristics can be improved. Core–shell MOFs can enhance stability and performance in electrocatalytic reactions, and this is achieved by coating the MOF surface with a more stable metal or substance. In the electrocatalytic hydrogen evolution reaction, MOF-based materials are highly recommended as superior building blocks for the creation of extremely effective electrocatalysts. To date, various electrocatalysts for HER, including pristine MOFs, MOFs with nanoparticles, MOF nitrides, MOF phosphides, and metal chalcogenides, result in excellent catalytic activity and stability.

Herein, we highlight an analysis of recent developments in MOFs and their composites with engineering features for hydrogen production. This article provides a brief history of MOFs and their characteristics, merits, limitations, applications, and enhancement techniques to boost electrocatalytic performance. In addition, for hydrogen generation applications, a thorough analysis of the morphological development and optimization techniques was conducted. Lastly, conclusions and suggestions for the future are offered to give guidance for further study in this area.

2. Reaction mechanism of the HER

The production of hydrogen through the hydrogen evolution reaction in alkaline media and a clean fuel alternative for different energy systems are currently areas of interest. There is an extra water dissociation phase in this process, which causes slow kinetics. Therefore, contemporary catalysts lose a lot of their catalytic activity in alkaline media and operate effectively in acidic ones. According to theoretical research, two primary criteria govern the catalyst's performance in an alkaline medium. These are the hydrogen binding energy and water dissociation. In general, the HER typically goes through two stages in an alkaline medium: the catalyst first breaks down an H_2O molecule into an adsorbed hydrogen atom and a hydroxyl ion (OH–) (H_{ads}, Volmer step). Next, a hydrogen molecule separates by combining two H atoms (Tafel step) or interacting with the water molecule (Heyrovsky step). Since each step contains a variety of adsorption intermediates, the catalyst should aid the reactions in both, making catalytic activity tuning challenging. The slow water dissociation step in alkaline media hinders catalytic activity, even for the most well-known catalyst, Pt, resulting in a reaction rate that is two to three orders of magnitude lower than that in acidic solution.

Therefore, in an alkaline medium, superior HER catalysis will be achieved by any catalyst that has a higher capacity to dissociate water molecules with a good binding capacity and create a hydrogen molecule. Few electrocatalysts that are comparable to Pt in an alkaline medium have been reported in terms of reaction efficiency. Thus, it is necessary to investigate the reaction process and confirm the fundamental principles of electrode kinetics. Even though this field of study has seen a lot of effort, industry and academia are beginning to improve the catalytic performance of the most advanced catalysts for the alkaline HER.

Generally, two electrochemical processes occur on two electrodes in electrocatalytic water splitting. Specifically, the anode electrode experiences the oxidation of water, whereas the cathode electrode experiences the reduction reaction of H_2O.[21,22] The HER is the primary reaction for producing hydrogen gas at the cathode. The process comprises the degradation of protons (H^+) to yield hydrogen gas (H_2).[23] The overall reaction for the HER is:

$$2H^+ + 2e^- \rightarrow H_2;$$

In a typical HER process, the protons are reduced at the cathode, where they gain electrons from the peripheral power source, forming hydrogen gas (H_2). In an acidic medium, the HER occurs in the subsequent three basic phases (Fig. 1);

2.1 Initial proton adsorption (Volmer step)

A proton (H*) from the solution of electrolyte adsorbs onto the catalyst's surface, where it is subsequently reduced by an electron to produce a hydrogen atom. This process is often termed the Volmer reaction.

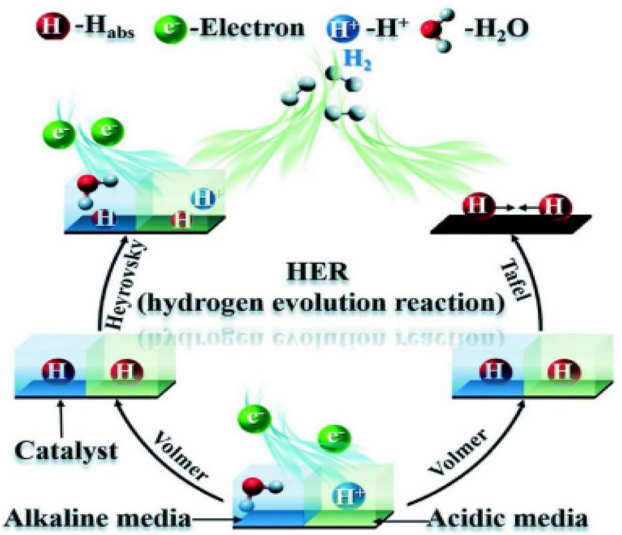

Fig. 1 Reaction involved in the HER process. Image is reproduced with permission from ref. 19 under Creative Commons Attribution License CC BY, Copyright © *CrystEngComm* 2020.

$$H^+ + e^- \rightarrow H_{ads}$$

where H_{ads} refers to the hydrogen atom that has been adsorbed onto the catalyst's surface.

2.2 Proton and electron coupling (Heyrovsky step)

In this stage, a proton (H^+) from the electrolyte and an electron (e^-) from an external circuit are linked to an adsorbed hydrogen atom (H_{ads}) to liberate a hydrogen molecule (H_2).

$$H_{ads} + H^+ + e^- \rightarrow H_2$$

This is often termed the Heyrovsky step, named after the scientist who first proposed it.

2.3 Bimolecular desorption (Tafel step)

In the Tafel step, two hydrogen atoms deposited on the catalyst's surface link to produce a hydrogen molecule, which is released from the catalyst's surface.

$$2H_{ads} \rightarrow H_2$$

3. Factors influencing the performance of the HER

The performance of the HER is influenced by the following factors;[24,25]

3.1 Overpotential and pH

The overpotential occurs when an applied voltage deviates from the equilibrium value. In electrochemical processes, for an appropriate catalyst, a low overpotential at a particular current density of 10 mA cm^{-2} needs to be considered. The electrolyte's pH also plays a significant role in the HER. Acidic conditions (low pH) generally favor the HER because protons are more readily available for reduction, but alkaline conditions (high pH) require more energy to generate hydroxide ions for proton reduction.[26]

3.2 Stability

Research on water-splitting mechanisms is typically conducted under harsh conditions, such as 0.5 M H_2SO_4 or 1 M KOH. Cyclic voltammetry is the most commonly used technique to assess the durability of electrocatalysts. High stability should be maintained in terms of overpotential, even after more than 5000 cycles. Remarkably, after 10 000 cycles, the current density often remains unchanged, suggesting perfect electrocatalytic performance. Additionally, chronoamperometry is used to monitor changes in current density changes over time at a fixed overpotential.[27]

3.3 Tafel slope

It has two significant connotations. First, the reaction kinetics are related to the Tafel slope. In electrochemical kinetics, a smaller

Tafel slope value indicates a faster rate. Second, we can forecast the electrochemical reaction process using the Tafel slope.

3.4 Surface area and morphology

A massive surface area is essential for improving electrocatalytic performance, as it delivers extra reaction sites. The catalyst's morphology, like nanoparticles, nanowires, and nanosheets, can influence the reaction sites and the efficiency.

3.5 Reaction kinetics

The rate-determining step (RDS) can vary depending on the catalyst. For Pt, the Volmer step is often the proportion-limiting step, while for non-metals, it might be the subsequent Tafel or Heyrovsky steps. A low activation energy for proton adsorption, bond breaking, and hydrogen desorption leads to faster HER rates and higher catalytic efficiency.

4. Structure of MOFs

The metal ions form coordination bonds with the ligands, typically through lone pairs of electrons from donor atoms in the ligands, like oxygen, nitrogen, *etc.* The metal–ligand bonds form coordination polymers with well-defined periodicity, resulting in a crystalline structure. The overall structure can be one, two, or three dimensions, contingent on the number and orientation of the metal–ligand bonds.[28] The coordination geometry of the metal centers, like octahedral, tetrahedral, square planar, or pyramidal, and the geometry of the ligands affect the porosity and functionality of the MOF.[29,30] Metal–organic frameworks (MOFs), which are composed of metal centers and organic linkers, are crystalline structures with homogeneous and adjustable nanometer-scale pores. These pores provide exceptional surface area and porosity. The pores' size and form can be tailored by modifying the organic linkers or metal centers. For instance, using larger linkers creates larger pores, while different metal ions influence the framework's connectivity.[31] The diversity of MOF structures and their tunability have made them highly versatile for the employment of gas storage and separation.[32] Their ordered and customizable architecture allows precise design for specific functions, as depicted in Fig. 2.

4.1 Metal ions or clusters in MOFs

These are typically transition metal ions like Co, Fe, Zn, or Al, or metal clusters, which serve as the nodes or coordination sites in the framework. These metal centers are often joined by organic ligands to constitute a three-dimensional structure. The commonly used metals in MOFs are:

(i) Transition metals: zinc (Zn), iron (Fe), cobalt (Co), *etc.*, are the most commonly used metals due to their ability to form stable coordination bonds with organic ligands.[33]

(ii) Lanthanides: some MOFs use rare-earth metals like cerium (Ce) or yttrium (Y) for specialized applications like luminescence or catalysis.[34]

(iii) Alkaline earth metals: magnesium (Mg) and calcium (Ca) can be used in MOFs, particularly for their role in creating highly porous materials.[35]

(iv) Metal clusters: in some MOFs, metal clusters like copper tetrahedra or iron-oxide clusters are used, which enhance stability and connectivity.[36,37]

4.2 Organic ligands in MOFs

Functional groups found in organic ligands allow them to work in tandem with metal ions to build the MOF structure's backbone.[38] These ligands are often multidentate, which means that they can bind to the metal through multiple points. The organic linkers are crucial for determining the size of the pores, symmetry of the structure, and functional groups in the framework. The versatility of the linker permits MOFs to exhibit a variety of structures, from rigid networks to flexible frameworks. The incorporation of functional groups can enhance the material's reactivity and its suitability for specific catalytic applications. Moreover, MOFs can be engineered with various functional groups attached to the organic ligands. These groups can impact specific properties of the MOF, such as hydrophilic or hydrophobic groups, which affect the ability of MOFs to adsorb water or organic solvents, aromatic rings or groups (for electronic or optical properties), and functionalized groups such as amino groups ($-NH_2$) for catalysis or chemical

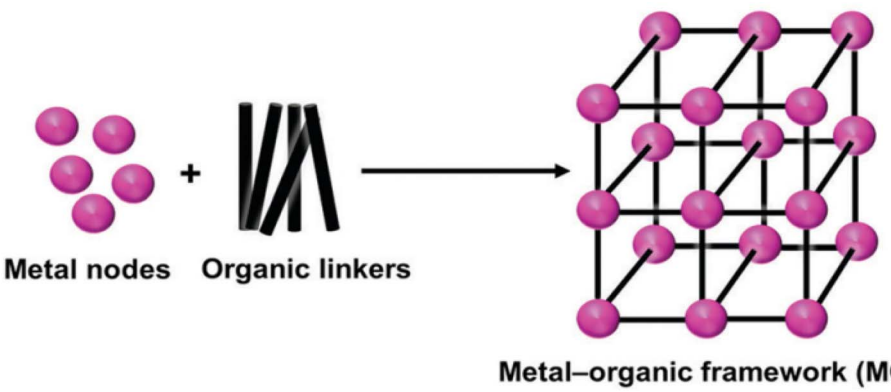

Fig. 2 Structure of a MOF. Image is reproduced with permission from ref. 25 under Creative Commons Attribution License CC BY, Copyright © *Nano-Micro Letters* 2020.

sensing.[39] The most commonly used ligands are carboxylates like terephthalic acid, phosphonates, or bipyridines. The commonly used organic ligands in MOFs are:

(i) Carboxylate-based ligands: ligands with carboxyl groups (–COOH) are the most common, where the oxygen atoms coordinate to the metal centers. Some examples of carboxylate-based ligands are terephthalic acid, phthalic acid, isophthalic acid, and fumaric acid.[40,41]

(ii) Bipyridine ligands: ligands like 2,2′-bipyridine, where nitrogen atoms coordinate to metals, are often used in combination with other ligands.[42,43]

(iii) Phosphonate ligands: these contain a phosphonic acid group ($–PO_3H_2$) and can form stable bonds with metals.[44]

(iv) Imidazole-based ligands: organic molecules like 2-methylimidazole, where nitrogen atoms coordinate with metals like Zn to form robust frameworks.[45,46]

(v) Aromatic or heterocyclic ligands: these ligands contain aromatic rings or heteroatoms like nitrogen, which act as coordination sites for the metals.[47]

5. Classification of MOFs

MOFs are categorized according to their dimensionality (1D, 2D, and 3D), topology, and connectivity of metal nodes and organic linkers[37,48,49] into:

(i) One-dimensional (1D) structures: these consist of linear chains where metal ions are linked by organic ligands.

(ii) Two-dimensional (2D) structures: the framework comprises sheets or layers, with ligands attaching to metal nodes to create a two-dimensional network.

(iii) Three-dimensional (3D) structures: these are the most common and involve the development of a three-dimensional network where metal ions are associated by organic linkers to create porous structures. This is the classic form of MOFs and is often referred to as a "Framework".

Also, MOFs are grouped according to the topology of their framework.[50,51] The framework can be highly diverse, and several common structures are:

(i) Cubic frameworks: some of the most common MOFs exhibit a cubic or octahedral symmetry, where metal centers are linked by organic ligands in a symmetrical pattern. Hexagonal frameworks: hexagonal MOFs consisting of organic linkers and metal centers are also frequently seen. These structures often have a high degree of symmetry and can form 2D or 3D networks.

(ii) Layered frameworks: some MOFs have 2D layered structures, where the metal centers and ligands form planar sheets stacked together. These materials are useful for applications requiring interlayer porosity or for the intercalation of guest molecules.

(iii) Open-framework structures: some MOFs are characterized by open frameworks where the network is highly porous, allowing for the inclusion of a wide range of guest molecules like gases or liquids.

6. MOF synthesis methods

Metallic ions and organic binders, referred to as "bridging ligands," are the two main components of MOFs, which feature a crystalline and porous network as given in Fig. 3(a). Numerous

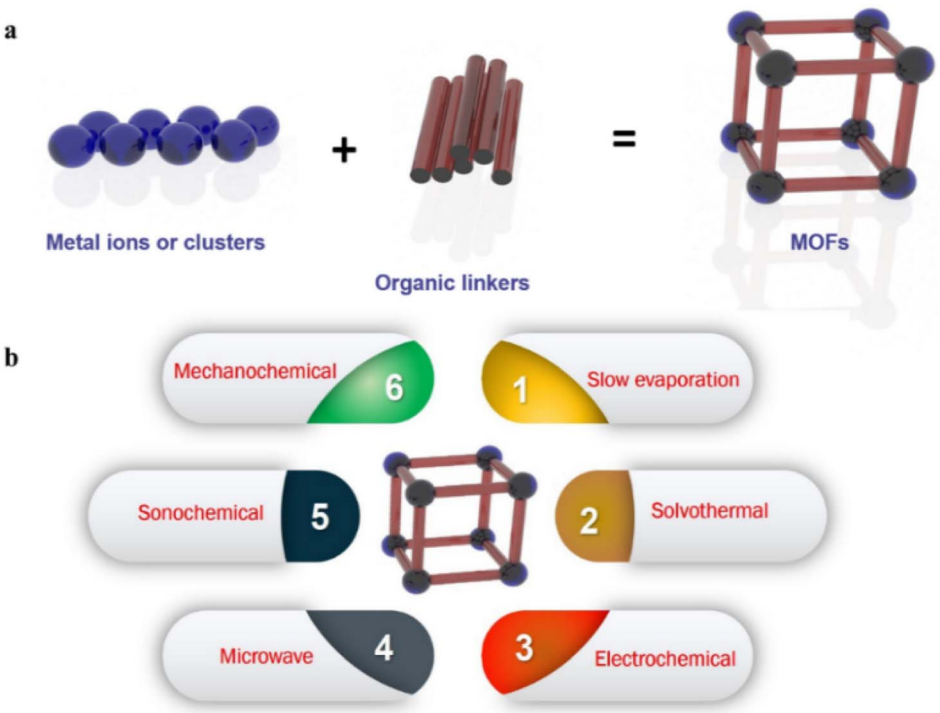

Fig. 3 (a) Diagrammatic illustration of MOF structures. (b) Techniques for MOF synthesis. The image is reproduced with permission from ref. 46 under Creative Commons Attribution License CC BY, Copyright © *Nano-Micro Letters* 2021.

preparation techniques[52] were used to create MOFs over the last 20 years, as shown in Fig. 3(b).

MOFs are synthesized using innumerable techniques, some of which are covered in this segment. In the solvothermal method, metal salts and organic ligands undergo dissolution in an appropriate solvent and are then heated for a while at elevated temperatures and pressurized in a Teflon-lined autoclave. This reaction can be referred to as solvothermal if water is employed. MOFs are created when the ensuing slurry exhibits nucleation and growth. Using the solvothermal method, MOFs like MOF-5,[53] MOF-74,[54] MOF-177,[55] ZIF-8,[56] and HKUST-1 (ref. 57) are synthesized under ambient conditions. Next, the hydrothermal method uses high pressure and temperature to start the formation of MOFs, just like the solvothermal method does. However, water was employed as the solvent instead of an organic one. The reaction mixture is also placed in a Teflon-lined autoclave for the controlled synthesis of MOFs. MOFs like Materials of Institute Lavoisier-101 (MIL-101) were synthesized through the hydrothermal method.[58] Other than solvothermal and hydrothermal methods of synthesis, utilizing microwave irradiation to expedite the synthesis process, which is also known as microwave-assisted synthesis, was a quick and effective process to produce MOFs like the University of Oslo-66 (UiO-66) by mixing the organic ligands and metal salts in a microwave reactor.[59] Rather than using water or organic solvents, MOFs were produced in an ionic solution. Although this approach uses specialized equipment, it is environmentally beneficial. The ionic liquid method is used to produce an MOF-like zeolitic imidazolate framework-7 (ZIF-7) by combining $Zn(NO_3)_2$ with 2-methylimidazole in an ionic solution, which is then heated to create a highly porous structure with adjustable characteristics.[60] Another quick and easy synthesis method is rapid liquid phase synthesis, which produces MOFs in the liquid phase. The collected liquid phase of the MOF product is then separated through filtration. Although it is a quick and easy process, hazardous solvents must be used. For instance, the Hong Kong University of Science and Technology-1 (HKUST-1) was synthesized through a rapid liquid phase method by combining $Cu(CH_3COO)_2$ and trimesic acid in a solution of acetic acid and water, and then filtering the mixture to get an extremely permeable and robust structure.[61]

7. Applications of MOFs towards the HER

MOFs are a sort of material that is formed from organic ligands and metal ions that combine to constitute a crystalline, porous structure. MOFs are being investigated more and more as electrocatalysts in a range of electrochemical uses, like batteries and water splitting, due to their special qualities.[62] In addition, numerous approaches have been put out and studied thus far for employing MOFs as raw materials for the generation of HER catalysts.[63] In this review, we have discussed the HER of several compounds such as MOF-derived metal phosphides, nitrides, metal dichalcogenides, metal oxide nanoparticles, single atoms, and their composites. Fig. 4 illustrates various approaches

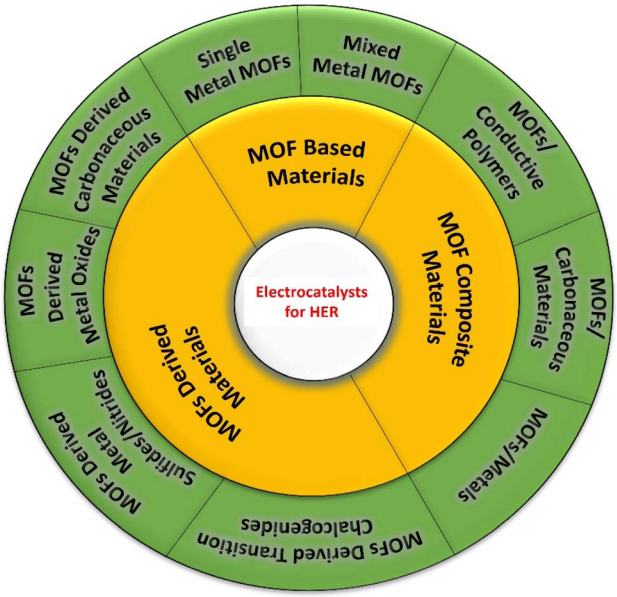

Fig. 4 Illustration of various MOFs, MOF-derived materials and their composites used as electrocatalysts for hydrogen production.

employed for MOFs for use as catalysts in the HER process. In some reactions, MOFs can demonstrate high catalytic efficiency, frequently approaching or even outperforming that of conventional catalysts like Pt. Compared to catalysts based on precious metals like Pt or gold, many MOFs use earth-abundant metals such as copper and nickel as active sites, which can lower costs.[64] The MOF's structure can be modified for particular uses, improving stability and performance in demanding electrochemical circumstances. By combining various metal centers in MOFs or adding functionalized ligands, the electrocatalytic capabilities of these materials can be improved.[65,66]

7.1 Single metal MOFs

MOFs were used in the pure form, just like other permeable constituents that are employed as catalytic agents. The framework configuration and catalytic activity are the foremost reasons for selecting the metal type and organic linkers for creating a pure form of MOFs for the HER. Yet, owing to proportional instability along with inadequate conductivity in acidic and alkaline circumstances, it has been rarely used as an electrocatalyst for HER catalysis. Several efforts have been made in this regard to increase the pristine MOF's catalytic activity for the HER without the need for post-treatment. Integration of a MOF with active constituents and its coupling with extremely favorable constituents like reduced GO, active carbon, and transition metal chalcogenides are discussed later. The two innovative, versatile Co MOFs (CTGU-5 and CTGU-6) described by Wu *et al.* may be preferentially condensed into pristine two or three-dimensional forms with the help of a neutral or anionic surfactant, respectively.[67] While an H_2O molecule exists in each polymorph, the way it bonds to the framework varies significantly, which influences the crystal structure and electrocatalytic ability of the HER. From the electrochemical studies, it

was revealed that the 2D CTGU-5 has much higher HER electrocatalytic activity than the 3D CTGU-6. Notably, AB & CTGU-5 (1 : 4) has the greatest HER efficiency of any MOF material because of its long-term stability, an immense current density of 8.6×10^4 A cm^2, and a lessened Tafel slope of 45 mV dec^{-1}. The 2D CO^{II} MOFs and conducting co-catalyst composite is established as a reliable and effective catalyst for the HER in acidic environments. Innovative three-dimensional nickel and cobalt redox active MOFs were developed using 4,4′-bipyridine ligands and ferrocenyl diphosphinate by Khrizanforova *et al.* and explored as an efficient electrocatalyst for the HER.[68] According to electrochemical research, a Ni-MOF (1) catalyst has reaction kinetics that are higher than those of a Co-MOF (2) catalytic agent. In particular, Ni-MOF has become the utmost dynamic non-noble metal-based molecular catalyst owing to its exceptional durability over time, limited Tafel slope of 60 mV dec^{-1}, and improved hydrogen evolution activity with an excessive potential of 350 mV at a current density of 10 mA cm^{-2}. A new 3D MOF with the formula $Co_2(Hpycz)_4 \cdot H_2O$ was synthesized by Zhou *et al.* and utilized as an active electrocatalyst for the HER. The prepared Co-MOF exhibits an excellent performance with an initial potential of 101 mV, a low Tafel slope of 121 mV dec^{-1}, long-term stability, and a current density of 1.62×10^{-4} A cm^{-2} respectively.[69]

Applying the Langmuir–Blodgett technique, Dong *et al.* prepared a huge and independent one-layer sheet of two-dimensional supramolecular polymer (2DSP) that contains triphenylene-fused nickel bis(dithiolene) complexes.[70] With a Tafel slope of 80.5 mV dec^{-1} and an overpotential of 333 mV at a current density of 10 mA cm^{-2}, these 2DSPs demonstrate exceptional catalytic sites for hydrogen evolution from water, outperforming carbon nanotube-supported molecular catalysts and heteroatom-doped graphene catalysts. Li *et al.* produced 2D polyhalogenated Co(II) coordination isostructural polymers using a simple and facile hydrothermal method.[71] He observed that the Co-MOF and acetylene black combination enhanced the hydrogen production reactivity in acidic media, and the Co–Cl_4-MOF's HER electrocatalytic activity was noticeably better than that of Co–Br_4-MOF and Co–F_4-MOF. Among all composites, the AB and Co–Cl_4-MOF (3 : 4) surprisingly show the highest HER action because of their long-term stability, lower Tafel slope of 86 mV dec^{-1}, and smaller overpotential of 283 mV at a current density of 10 mA cm^{-2}. The electrochemical methodology used catalysts based on nickel metal to produce hydrogen. But their poor activity limited their use in the catalysis industry. There have been several methods reported for improving the HER's electrocatalytic performance.[25] Initially, using a pyrolysis technique, Wang *et al.* produced nickel NPs over the carbon form Ni-MOF for deployment in the HER.[72] The surface of Ni metal was modified using NH_3 gas. According to the findings, Ni nanoparticles produced at 0.4 bar of pressure had a low overvoltage of 88 mV at 20 mA cm^{-2}.

7.2 Mixed-metal MOFs

Next, using direct pyrolysis of MOFs, Zhao *et al.* first revealed the linked development of two distinct catalytic sites (SA-Co and Co@C–N sites) from Zn/Co-MOF.[73] They illustrate sulfur-assisted pyrolysis for dual-site dissociation and SA-Co site refinement. Thus, a dual metal-site decoupling technique and the findings of single-atom electrocatalysis in MOF-derived materials are crucial for the logical progress of noble metal-free catalytic agents, which had a beneficial impact on both electrochemical reduction of oxygen and hydrogen. Fig. 5 shows the decoupling process and the linked evolution of metallic and single-atom cobalt sites.

ZIF-67/$Cu(OH)_2$ was calcined to produce bimetallic Cu, Co nanoparticles over a carbonaceous framework (CuCo@NC). The outcome demonstrates that CuCo@NC has outstanding catalytic capabilities, exhibiting an overpotential of 145 mV at 10 mA cm^{-2}, which is given in Fig. 6(a–d). This CuCo@NC electrocatalyst greatly improves electrocatalytic performances in the

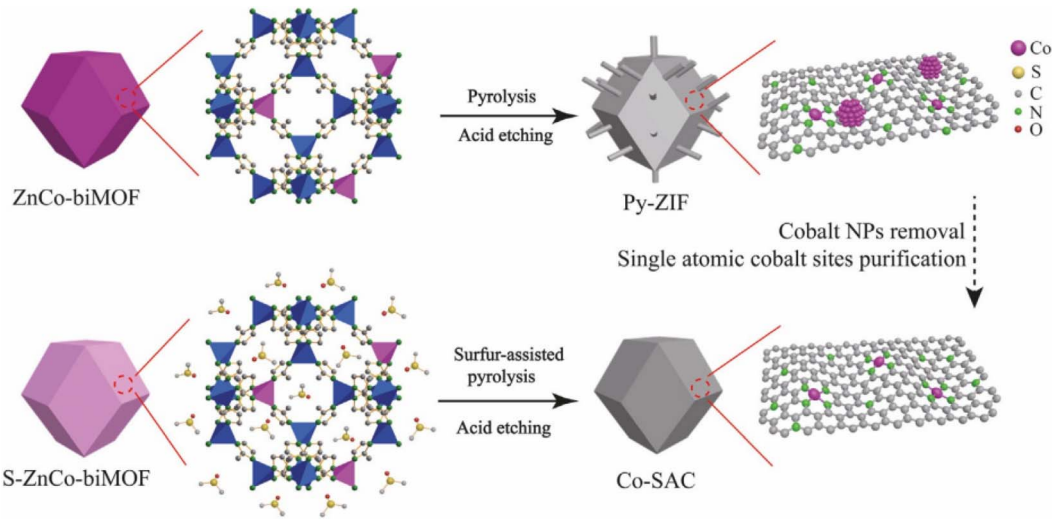

Fig. 5 The decoupling process and the linked evolution of metallic and single Co sites. The image is reproduced with permission from ref. 68 under Creative Commons Attribution License CC BY, Copyright © *ChemSusChem* 2018.

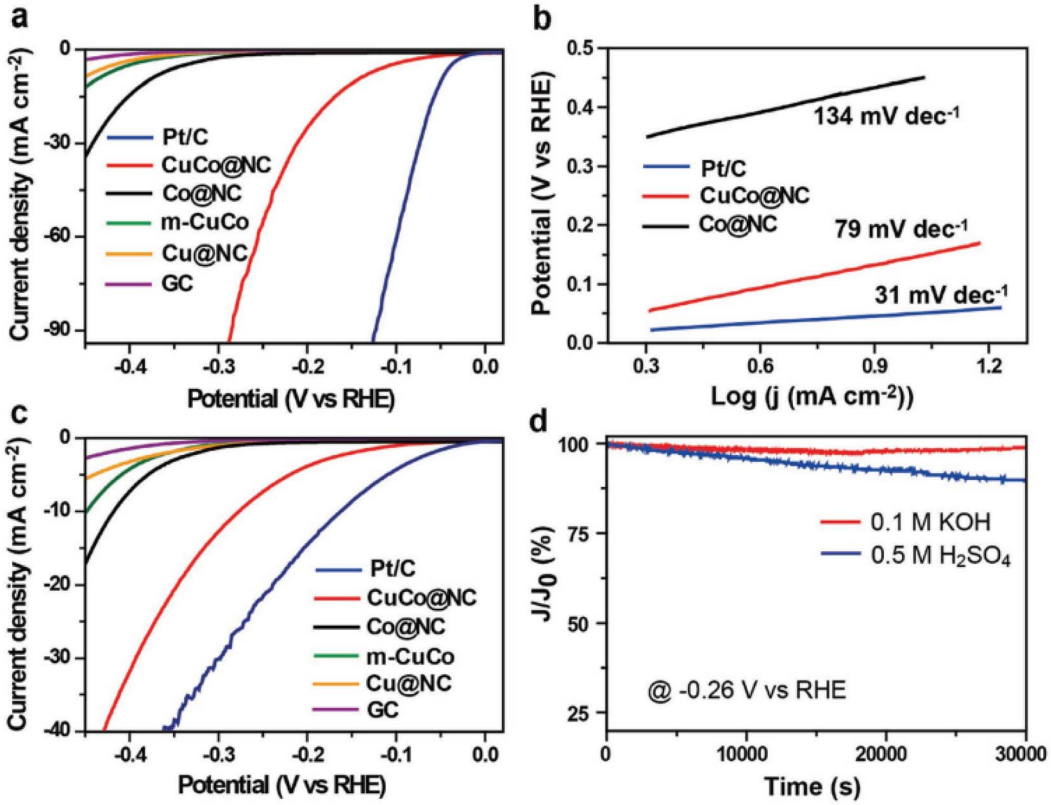

Fig. 6 (a) LSV curves for hydrogen evolution in 0.5 M of H_2SO_4 for several samples, (b) corresponding Tafel curves, (c) LSV curves displaying hydrogen evolution in 0.1 M of KOH for different samples, and (d) CuCo@NC's HER stability tests in 0.5 M of H_2SO_4 and 0.1 M of KOH. The image is reproduced with permission from ref. 69 under Creative Commons Attribution License CC BY, Copyright © *Advanced Energy Materials* 2017.

HER by offering a large number of catalytic sites, substantial nitrogen mixing, robust synergistic interaction, and enhanced mass transfer.[74]

7.3 MOF-derived metal oxide nanoparticles

Although the evolution of hydrogen in alkaline media was an objective for the environmentally friendly growth of hydrogen as a sustainable substitute for different energy sources, its kinetics are slow because of the extra water dissociation phase.[75] Thus, cutting-edge catalysts that function effectively under acidic conditions significantly worsen in alkaline media. Finding effective non-noble catalysts equivalent to platinum catalysts in alkaline electrolytes is challenging. Thus, creating advanced electrode components for the HER in water-alkali remains a difficult endeavor. Later, the development of metal oxide on a metal substrate was known to enhance the HER's catalytic activity in an alkaline solution. Based on this, Jing Wang *et al.* synthesized NiO_x@bamboo-like carbon nanotube hybrids (NiO_x@BCNTs) by a simple technique and employed them as a vigorous HER catalyst in the electrocatalytic process.[76] They reported that, in alkaline solution, the hybrids showed exceptional catalytic activity and significant durability. At an overpotential of about 79 mV, a benchmark HER current density of 10 mA cm^{-2} had been attained. For the first time, this unquestionably confirms, in conjunction with the experimental findings and DFT computations, that the exceptional catalytic activity is mostly due to the intrinsically higher Ni^0 ratio on the Ni/NiO interface. Bai and colleagues conducted another study on metal/metal oxide from a MOF substrate. According to that, Bai successfully developed a composite structure using a MOF-routed technique that partly oxidized cobalt NPs embedded in nitrogen-doped carbon typical dodecahedral frameworks (Co@Co_3O_4-NC).[77] Fig. 7(a–d) depicts the two-electrode water splitting and gas collection device, polarization graphs of Co@Co_3O_4-NC‖Co@Co_3O_4-NC, Pt/C‖IrO_2, Pt/C‖Pt/C and IrO_2‖IrO_2, stability investigation of Co@Co_3O_4-NC before and after 3000 CV cycles at 50 mV s^{-1} and volume of generated H_2 and O_2 at a constant potential of 2 V. The result shows that the metallic cobalt interior core transfers the distinct ions straight to the nitrogen–carbon structure, while the Co_3O_4 layer functions as an effective charge-separation functional layer. Its distinct structure allows for a faster charge separation/transport process, which significantly increases electrocatalytic activity. Consequently, it was shown that Co@Co_3O_4-NC was a bi-functional electrocatalyst that performed better than single Pt or IrO_2 electrodes in terms of stability and catalytic activity.

7.4 MOF-derived metal phosphides/nitrides

Transition metal phosphides (TMPs) were thought to be extremely effective electrocatalysts with remarkable potential to

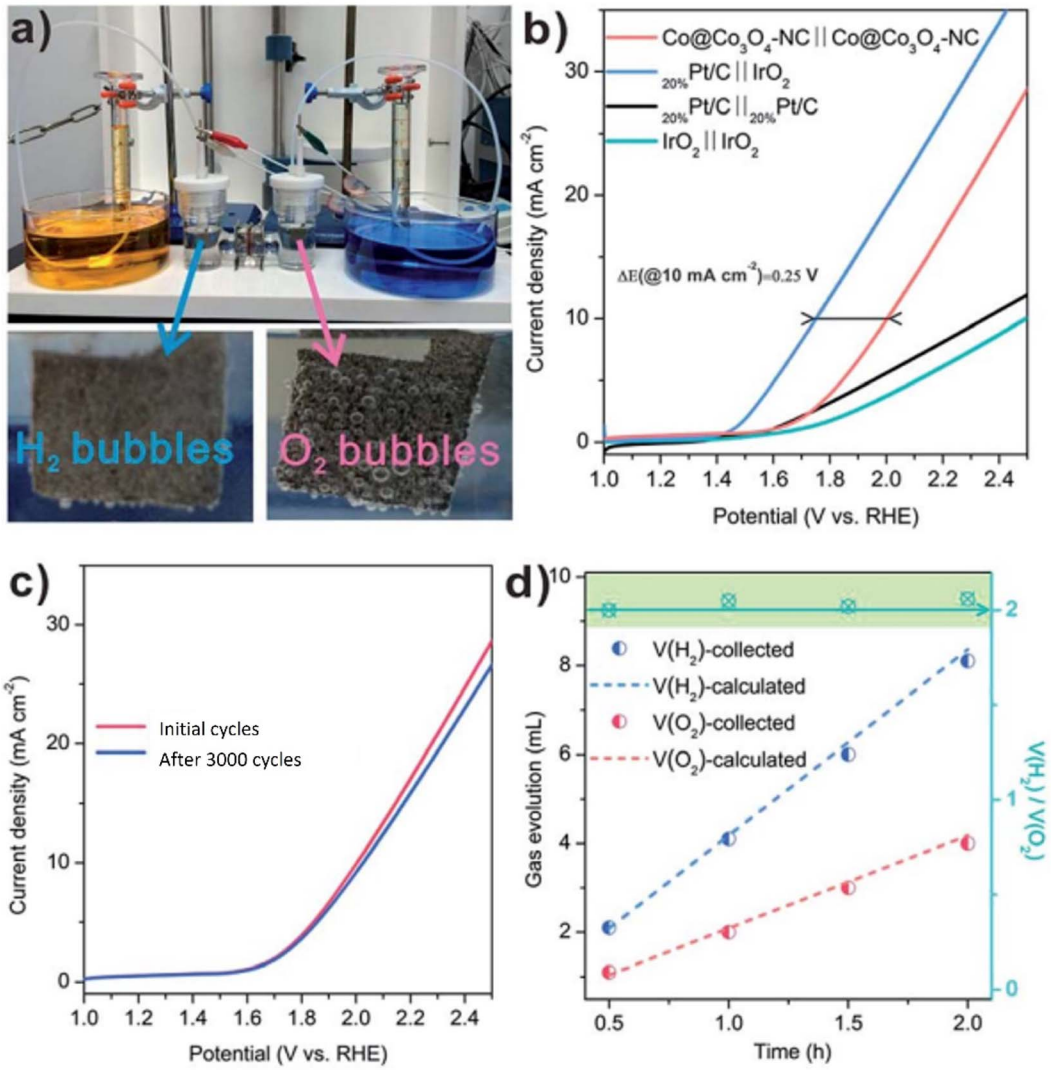

Fig. 7 (a) Photograph of the two-electrode water splitting and gas collection device. (b) Polarization curves of Co@Co_3O_4-NC||Co@Co_3O_4-NC, Pt/C||IrO_2, Pt/C||Pt/C and IrO_2||IrO_2. (c) Stability test of Co@Co_3O_4-NC before and after 3000 cycles at 50 mV s^{-1} (d) Volume of generated H_2 and O_2 at a constant potential of 2 V. Image is reproduced with permission from ref. 72 under Creative Commons Attribution License CC BY, Copyright © *Journal of Materials Chemistry A* 2013.

alleviate the energy crisis. They have also been a growingly popular source for energy conversion and storage devices. Wang *et al.* first synthesized zeolitic imidazole framework-67 (ZIF-67) polyhedra *via in situ* on commercial melamine foam fibrils at room temperature.[78] They are subsequently carbonized and phosphidized to create the hierarchical CoP@N-doped carbon hybrid foam (CoP@NC/CF), with an interrelated construction. In addition to preventing CoP nanoparticle aggregation, the three-dimensional interconnected carbon networks offer effective and quick pathways for the rapid flow of electrons and ions. Thus, exceptional HER activity with a low Tafel slope of 64.8 mV dec^{-1}, a low overpotential of 151.3 mV at 10 mA cm^{-2}, and outstanding durability is made attainable by the exceptional architecture of CoP@NC/CF. Additionally, stable HER electrode materials are made from MOFs in acidic and alkaline media. Pan *et al.* reported a new hybrid nanostructure by pyrolysis–oxidation–phosphorization based on core–shell ZIF-8@ZIF-67, in which CoP NPs are implanted in a nitrogen-doped carbon nanotube hollow polyhedron (NCNHP).[79] He added that a potential as low as 1.64 V was required to reach a current density of 10 mA cm^{-2} when CoP/NCNHP was utilized as an exceptional electrode for water splitting. Even after 36 hours of continuous use, with almost no potential decay, CoP/NCNHP showed superior activity.

In addition, Ji *et al.* investigated TMP-based catalysts for the HER.[80] In this study, he synthesized CoP nanoframes (CoP NFs) through precipitation and chemical etching, followed by a lower-temperature phosphidation method. The SEM, TEM, HRTEM, and EDAX images of CoP NFs are displayed in Fig. 8(A–G). With a current density of 10 mA cm^{-2} and a cell voltage of just 1.65 V, CoP NFs produce exceptional bifunctional catalysts for the HER and OER, hence providing a very effective water electrolyzer. He also extended the method to make Co dichalcogenide (CoX_2) nanoframes by considering X = S, Se, and Te,

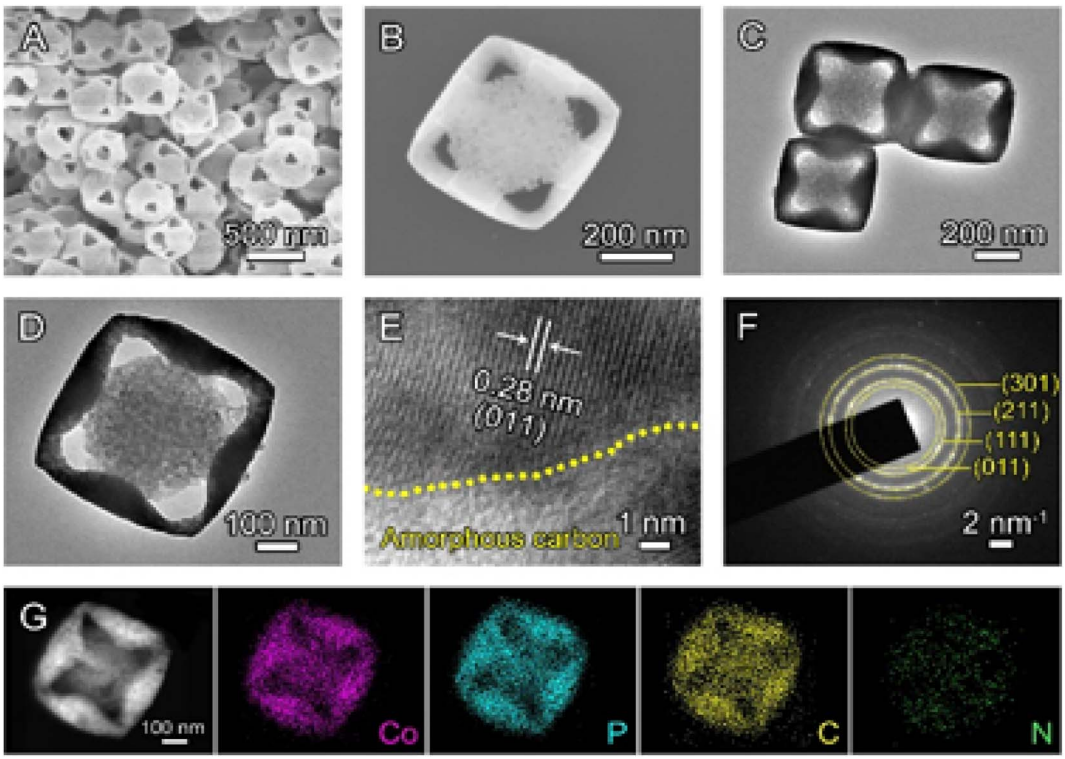

Fig. 8 The SEM images (A and B), TEM images (C and D), HRTEM images (E), SAED pattern (F), and TEM EDAX (G) for CoP NFs. The image is reproduced with permission from ref. 75 under Creative Commons Attribution License CC BY, Copyright © *ACS Catalysis* 2020.

respectively. HER activity is according to the following sequence, according to the results of electrochemical tests confirmed by DFT calculations: CoP NFs > $CoSe_2$ NFs > CoS_2 > $CoTe_2$ NFs. Long Jiao *et al.* studied a layered CoP/reduced graphene oxide (rGO) composite that has been effectively generated by pyrolysis and a subsequent phosphating procedure using a logically constructed sandwich-type metal–organic framework/graphene oxide as a template and precursor.[81] In acid solution, the resulting CoP/rGO-400 shows outstanding HER activity.

Wang *et al.* reported the production of controlled spongy Ni_2P nanosheets with NiO-MOF-74 as intermediates and a traditional phosphorization technique.[82] In the HER, the spongy Ni_2P NSs demonstrated outstanding catalytic behavior with quite a low Tafel slope of 63 mV dec^{-1} and a low overpotential of 168 mV at a current density of 10 mA cm^{-2} in 1.0 M KOH. This result is due to the electron conduction channels made possible by the porous architectures of Ni_2P nanosheets, which speed up the dispersion of H_2 and O_2 bubbles on the electrode and enable electron transfer. In another study, Suqi He and his co-workers used a modest and rapid microwave-assisted process for the synthesis of MOF-74-Ni. They utilized it as a substrate to produce a permeable hybrid Ni_2P/C.[83] In the HER process, the prepared Ni_2P/C demonstrated outstanding electrocatalytic performance with a poor starting potential of −94 mV, stability (>24 h), and a Tafel slope of 113.2 mV dec^{-1}. The outstanding performance has been ascribed to the huge superficial area due to the porous framework, inherently increased electrocatalytic behavior of Ni_2P, and elevated electrical conduction from the carbonaceous elements. Tian *et al.* synthesized nickel phosphide nanoparticles through a solid chemical transformation method, using Ni-BTC MOF as a precursor under moderate conditions.[84] The prepared sample was examined through XRD studies to confirm the formation of Ni_2P nanoparticles, which are shown in Fig. 9(a). The surface morphology, the spectrum of elemental mapping, the HRTEM image, equivalent line characteristics, and FFT patterning of the Ni_2P NPs are given in Fig. 9(b–g). With a reduced potential of 75 mV and an improved current density, these affordable, earth-abundant MOF-derived Ni_2P NPs showed excellent electrocatalytic behavior for the process of HER. Their performance is constructively comparable to that of metal phosphides, indicating a cheap substitute for expensive Pt catalysts in real-world practice. Furthermore, this preparation approach is straightforward, adjustable, affordable, and versatile, making it extremely promising for large-scale manufacturing. This approach was expanded to include the broad synthesis of more TMPs from MOFs. In addition, Tian and his co-workers used a solid-state interaction involving Ni-BTC and NaH_2PO_2 to produce Ni_2P and $Ni_{12}P_5$ nanopowder. In terms of hydrogen generation, Ni_2P performed better than $Ni_{12}P_5$.[85]

Feng *et al.* used a practical and simple synthesis method for developing fibrous rod-like cobalt–nickel bimetal nitride using a bimetal–organic framework precursor.[86] The prepared Co_xNi_yN exhibits a high surface area, abundant mesoporous structure, and uniformly distributed metal active sites. Furthermore, the

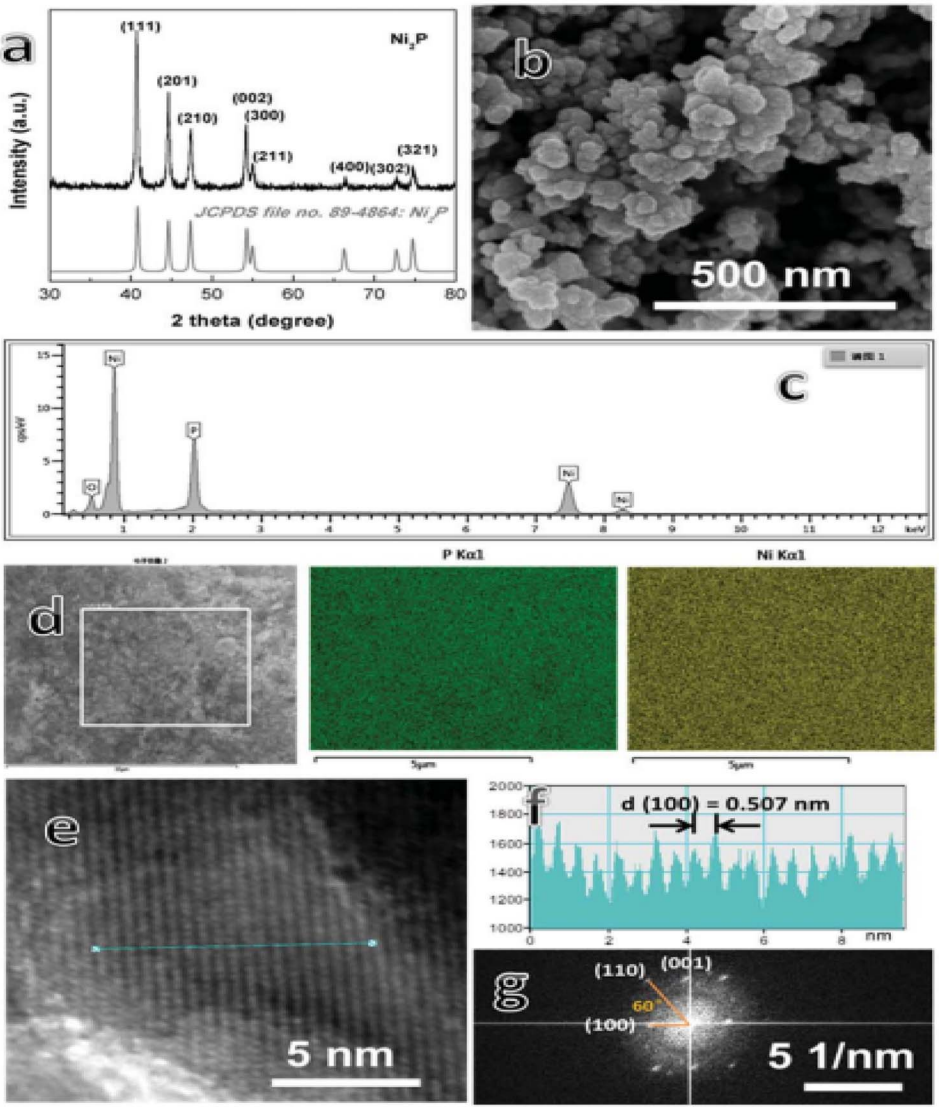

Fig. 9 (a) XRD, (b) SEM, (c) EDS spectrum, (d) SEM-mapping, (e) HRTEM, and (f and g) equivalent line profile and FFT pattern of the Ni_2P NPs. Image is reproduced with permission from ref. 78 under Creative Commons Attribution License CC BY, Copyright © *RSC Advances* 2015.

presence of Ni results in abundant active sites and changes the Co atom's electrical surroundings. From Fig. 10(A–F), it was shown that, in an all-pH environment, porous Co_2Ni_1N exhibits outstanding stability and strong catalytic activity, with weak overpotentials of 102.6, 92.0, and 152.8 mV at a current density of 10 mA cm^{-2} in various solutions, respectively.

7.5 MOF-derived transition metal chalcogenides

Due to their appropriate hydrogen adsorption-free energy, transition metal dichalcogenides (TMDs) were valued in the electrochemical method of producing hydrogen. However, the use of TMD-based catalysts for the HER offers a difficult task in durability. TMDs generated from MOFs showed a promising role in the growth of long-lasting and active HER. A composite of Fe/$CoSe_2$ embedded in N-doped carbon (Fe–$CoSe_2$@NC) was prepared by Wu *et al.* through selenization of Fe^{3+}-etched MOF (ZIF-67).[87] With a limited Tafel slope of about 40 mV dec^{-1} and a modest overpotential of −143 mV at 10 mA cm^{-2}, the Fe–$CoSe_2$@NC hybrid demonstrated improved HER performance because of the electrical and morphological structure. It also exhibited superior faradaic efficiency and good stability. The increased active surface area brought on by the etching of Fe^{3+} ions may be the cause of the increased HER activity. Zhou *et al.* developed $CoSe_2$ NPs encapsulated in carbon nanotubes ($CoSe_2$@DC). Co-based MOFs underwent a carbonization and the selenium degradation process. As a key step in adding more defects to carbon nanotubes, the pre-oxidation treatment facilitated the interaction between selenium and Co@carbon and improved HER performance.[88] An inferior potential of −40 mV *vs.* RHE, a small Tafel slope of 82 mV dec^{-1}, a high current density (132 mV, 10 mA cm^{-2}), and strong catalytic stability in 0.5 M H_2SO_4 were all characteristics of the prepared $CoSe_2$@DC which exhibits superb catalytic activities as shown in Fig. 11(a–f).

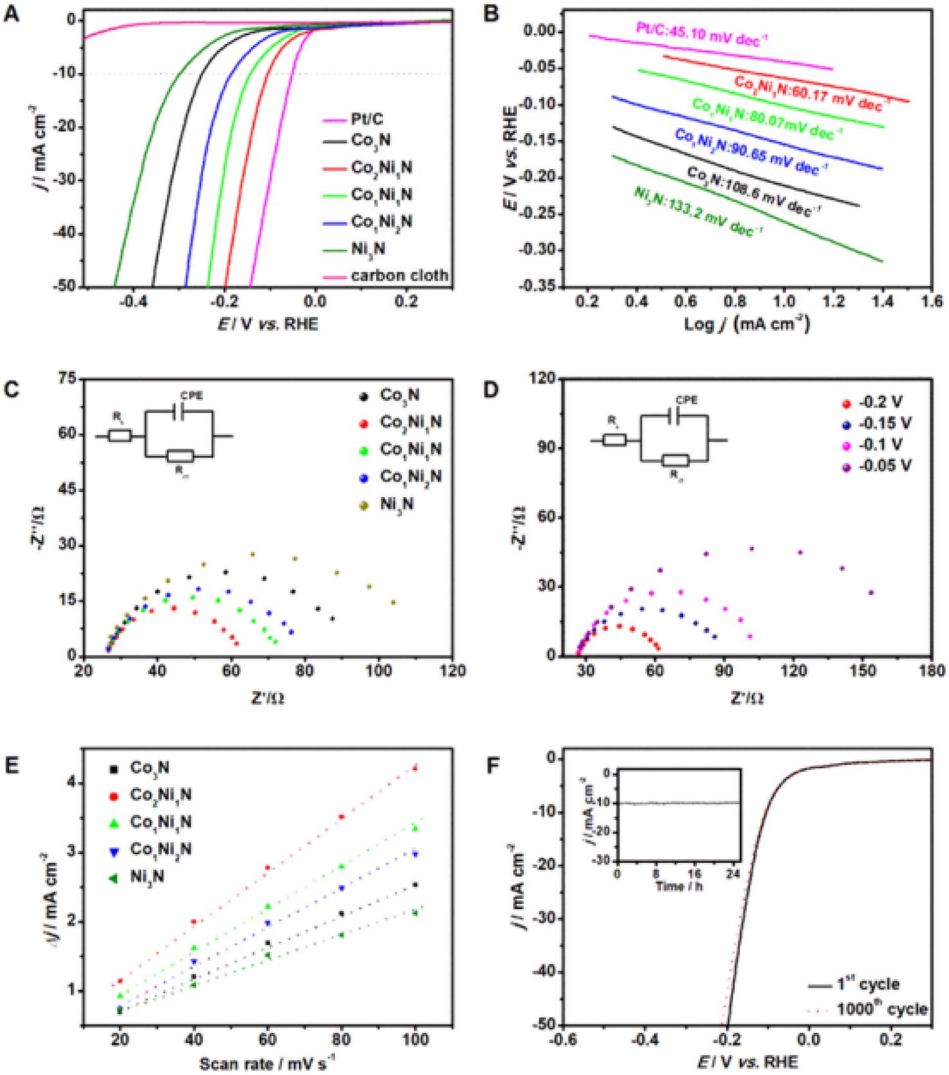

Fig. 10 (A) LSV polarization graph of Pt/C, bare carbon cloth, Co_3N, Co_2Ni_1N, Co_1Ni_1N, Co_1Ni_2N, and Ni_3N in 1.0 M KOH solution at 5 mV^{-1}. (B) Tafel plots of Pt/C and Co_xNi_yN materials. (C) EIS Nyquist plot of Co_3N, Co_2Ni_1N, Co_1Ni_1N, Co_1Ni_2N, and Ni_3N from 10 mHz to 100 kHz (inset: the equivalent circuit. R_s and R_{ct} correspond to the electrolyte and charge transfer resistance, respectively). (D) EIS Nyquist plots of Co_2Ni_1N from 10 mHz to 100 kHz at various potential levels. (E) Capacitive currents against the scan rate for Co_xNi_yN materials. (F) Polarization curves of Co_2Ni_1N before and after 1000 CV sweeps (inset: time dependence on current density for Co_2Ni_1N). Image is reproduced with permission from ref. 79 under Creative Commons Attribution License CC BY, Copyright © *Applied Materials* 2019.

Pyrite $NiSe_2$ has recently been regarded as a promising HER catalyst because of its superior conductivity, robust corrosion resistance, and affordability. $NiSe_2$'s HER performance in alkaline electrolytes remains unsatisfactory, which may be due only to activated water dissociation in alkaline media.[89] Using this perception, Liu *et al.* described the fabrication of new electrocatalysts of $Ni(OH)_2/NiSe_2$ NS on carbon cloth, which has exceptional catalytic activity with an inferior potential of 82 mV to exhibit a current density of 10 mA cm^{-2} and maintains stability for 12 h in 1.0 M KOH.[90] This is higher than that of the most recently developed $NiSe_2$/CC electrocatalysts. For the first time, Zhou *et al.* established a strategy for growing $NiSe_2$ on conductive nickel foam to produce a three-dimensional fibrous $NiSe_2$/Ni material by thermal selenization of commercially existing Ni foams.[91] This approach for material fabrication is inexpensive and time-efficient, with the minimal cost of nickel foam. Despite the straightforward procedure, the grown $NiSe_2$/Ni catalysts exhibit magnificent electrochemical stability, significant cathodic current densities of 100 mA cm^{-2} at −143 mV, and lower Tafel slopes of about 49 mV dec^{-1}. On considering the primary transition metal dichalcogenide-based catalysts, Zhou *et al.* described permeable $NiSe_2$ catalysts that are better for water electrolysis.[92] $NiSe_2$ displays HER performance comparable to the most advanced platinum catalysts. They developed $NiSe_2$ directly from commercial nickel foam using surface roughness engineering aided by acetic acid. To enhance the TMD performance, Wang *et al.* utilized first-principles estimation for performing efficient studies of the relationship between transition metal doping and $NiSe_2$ catalytic activity.[93] He confirms the formation of $Ni_{1-x}Fe_xSe_2$ porous

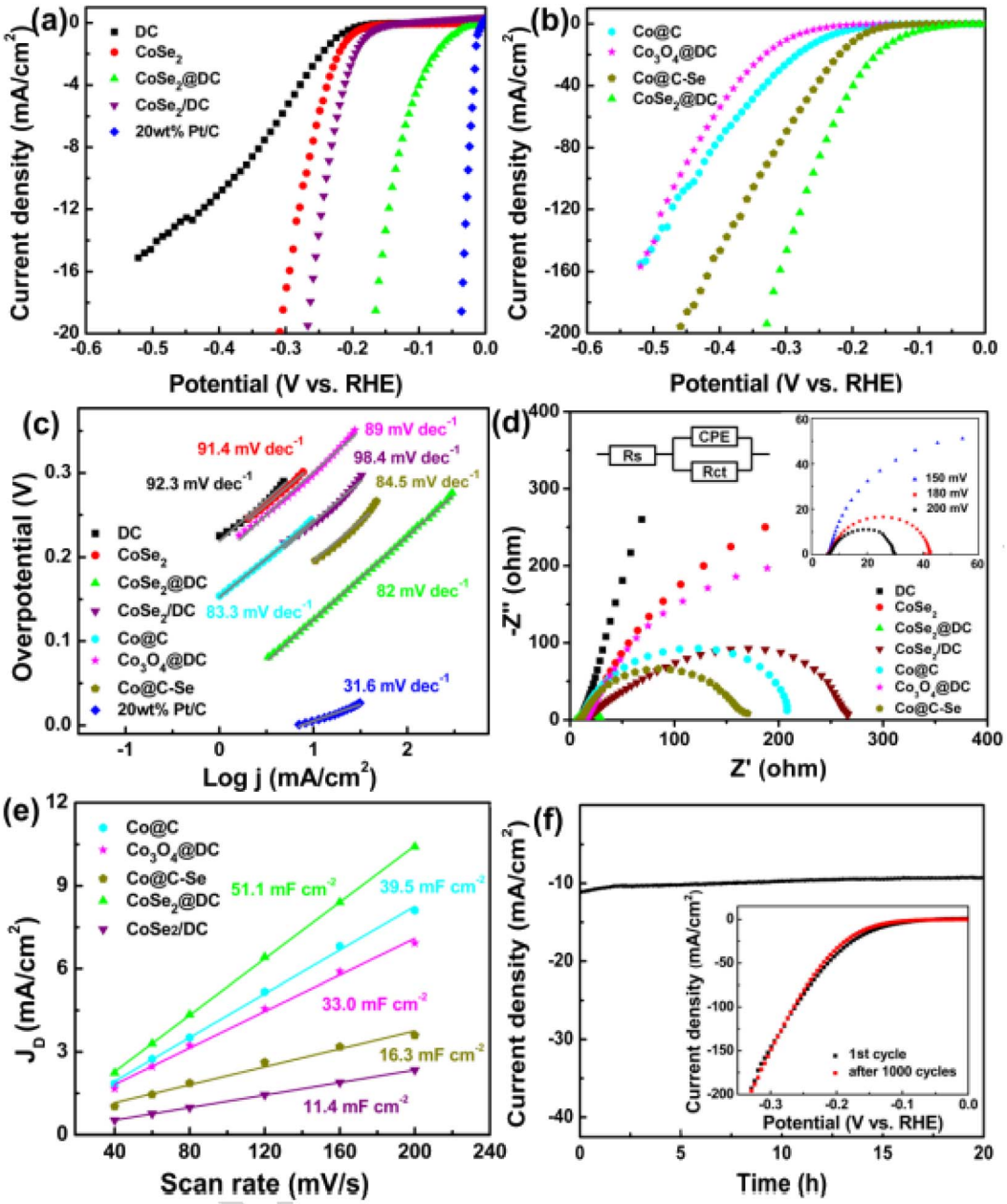

Fig. 11 (a) Polarization curves of DC, $CoSe_2$, $CoSe_2$/DC, $CoSe_2$@DC, and 20 wt% Pt/C without *IR* correction. (b) Polarization curves of Co@C, Co_3O_4@DC, $CoSe_2$@DC and Co@C–Se. (c) Tafel plots from (a and b). (d) Nyquist plots of different samples using modified electrodes that have an overpotential of 200 mV. The equivalent circuit and Nyquist plots of $CoSe_2$@DC modified electrodes with varying overpotentials are shown in the inset figure, (e) the capacitive currents as a function of scan rates, and (f) the chronoamperometric response for $CoSe_2$@DC. The inset figure shows the polarization plots of $CoSe_2$@DC before and after 1000 cycles. The image is reproduced with permission from ref. 81 under Creative Commons Attribution License CC BY, Copyright © *Nano Energy* 2016.

NSs grown on CFC through XRD and Raman spectroscopy. The structural morphology of as-prepared various combinations of $Ni_{1-x}Fe_xSe_2$ porous NSs grown on CFC was examined by SEM and HRTEM, and their corresponding elemental mapping images showed the formation of $Ni_{1-x}Fe_xSe_2$ porous NSs grown on CFC. From the results, it is shown that Fe is the ideal element to modify $NiSe_2$'s electrocatalytic activity with reduced ΔGH* values and enhanced electrical conductivity. Fe/$NiSe_2$ NSs are successfully produced on carbon cloth to offer additional experimental support. When comparing these nanosheets to their undoped counterparts, the efficiency of the hydrogen evolution reaction is noticeably higher. At a reduced overpotential of 64 mV, the optimized $Ni_{0.8}Fe_{0.2}Se_2$ electrocatalysts produce a current density of 10 mA cm^{-2} with extraordinary stability, as shown in Fig. 12(a–f).

Other than nickel and cobalt-based catalysts, $MoSe_2$ nanosheets are thought to be potential electrocatalysts for the HER. However, due to significant aggregation or restacking of $MoSe_2$ nanosheets, the manufacturing of $MoSe_2$ electrodes for extensive industrial use remains complex. Recently, it was found that

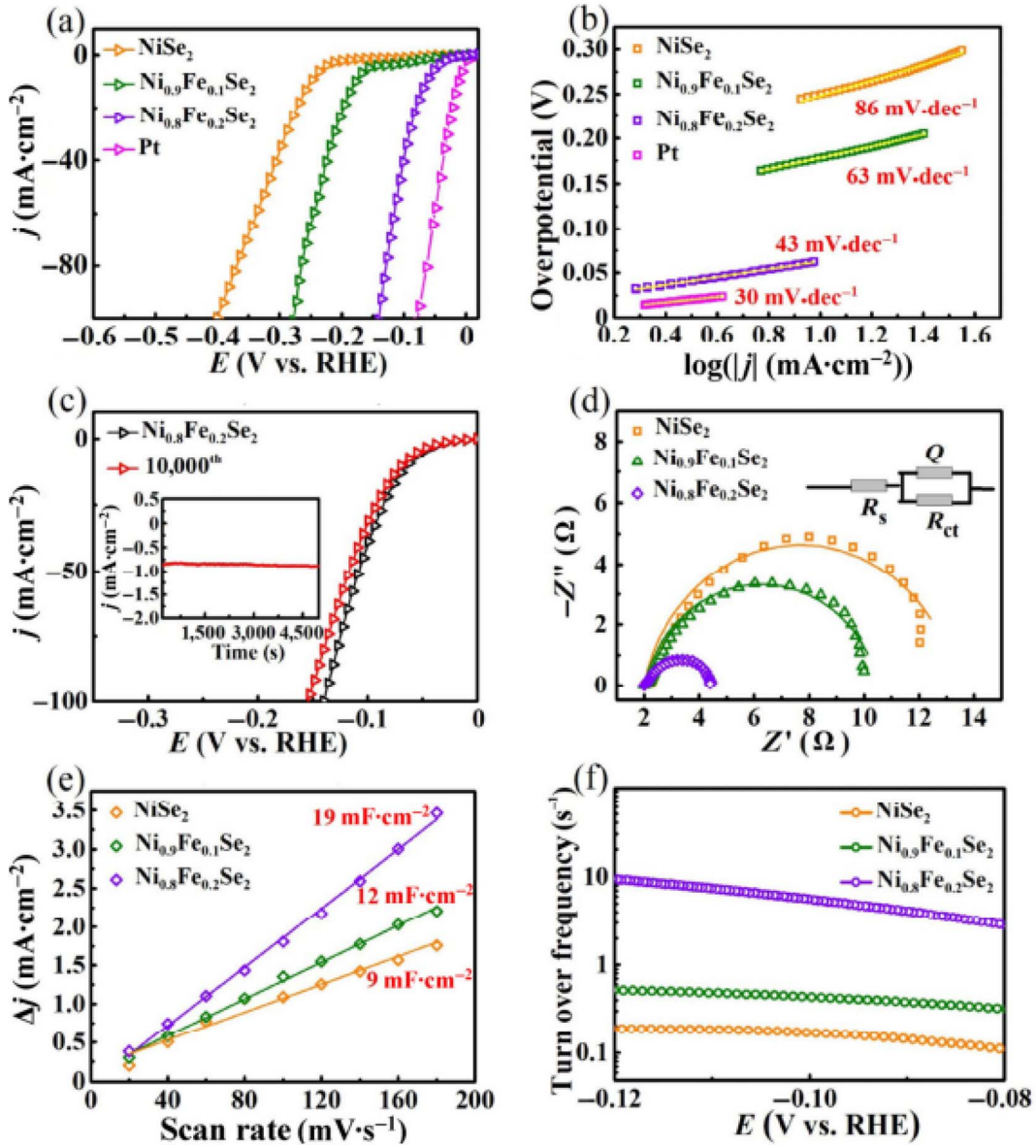

Fig. 12 (a) Linear sweep voltammetry curves and (b) Tafel plots for $NiSe_2$/CFC, $Ni_{0.9}Fe_{0.1}Se_2$/CFC, $Ni_{0.8}Fe_{0.2}Se_2$/CFC, and Pt/C measured in 0.5 M of H_2SO_4, (c) current density curve with time (inset) and LSV graphs before and after a stability test of 10 000 cycles for $Ni_{0.8}Fe_{0.2}Se_2$/CFC, (d) EIS Nyquist plots measured at −0.4 V *vs.* RHE and the lines fitted by using equivalent electrical circuits (inset) of Pt and $Ni_{1-x}Fe_xSe_2$/CFC, (e) double-layer capacitances of $Ni_{1-x}Fe_xSe_2$, and (f) H_2 turn over frequencies (TOFs) per surface site over different catalysts. Image is reproduced with permission from ref. 86 under Creative Commons Attribution License CC BY, Copyright © *Nano Research* 2018.

3D hierarchical constructions worked well to overcome this obstacle. Carbon fiber paper (CFP) was used to construct independent hierarchical structures for electrocatalysts because of its porous structure, extreme electrical conduction, strong mechanical stability, and exceptional corrosion impedance in acidic and alkaline solutions. Based on this idea, $MoSe_2$ NSs transversally oriented on SnO_2 nanotubes were constructed by Huang *et al.*, to improve the amount of unveiled active edges of $MoSe_2$.[94] This resulted in a reduction of the Tafel slope of $MoSe_2$@SnO_2 NTs to 51 mV dec^{-1} from 70 mV dec^{-1} of $MoSe_2$ and reduction of the overpotential at a current density of 10 mA cm^{-2} to 0.174 V (*vs.* RHE) from 0.247 V. Despite the increased performance, the electron transport from the electrode to the catalysts is limited by weak conductivity of SnO_2 NTs. Therefore, using templates with higher conductivity could enhance the activity even further. On highly conductive $NiSe_2$ porous foam, Zhou *et al.* produced $MoS_{2(1-x)}Se_{2x}$ particles, which showed significantly improved electrochemical characteristics as depicted in Fig. 13(a–e). According to DFT calculations, the ΔGH on $MoS_{2(1-x)}Se_{2x}$/$NiSe_2$ in (100) and $MoS_{2(1-x)}Se_{2x}$/$NiSe_2$ in (110) planes were reduced from 8.4 kcal mol^{-1} on $MoS_{2(1-x)}Se_{2x}$ to 2.7 kcal mol^{-1} and 2.1 kcal mol^{-1}, respectively.[95] Hence, $MoS_{2(1-x)}Se_{2x}$ and $NiSe_2$ work in concert to significantly increase electrocatalytic activity. This work inspired Zhang *et al.* to believe that the catalytic performance of highly conductive $NiSe_2$ and 2D $MoSe_2$ nanosheets may be significantly enhanced

by integrating them into a 3D self-standing hierarchical framework. He synthesized 3D hierarchical $MoSe_2/NiSe_2$ NWs arrays through a two-step hydrothermal technique, which exhibits a Tafel slope of 46.9 mV dec^{-1} with a small overpotential of 249 mV respectively.[96]

MOF-driven metal sulfides were assessed as competitors for modifying the platinum in the water-splitting process, much like the metal selenides. Guan *et al.* proposed a logical design for new CoS_2 nanotube arrays that are put together on a flexible support and may be used right away as a very dynamic bifunctional electrocatalyst for the water-splitting process.[97] At the very first moment, uniform wire-like MOF nanoarrays were developed, and then the MOF arrays were converted into CoS_2 nanotube arrays by a sulfidation procedure using heat treatment. With a cell voltage of 1.67 V and the use of CoS_2 nanotube arrays as catalysts, a water-splitting current density of 10 mA cm^{-2} in an alkaline solution is attained. The steady current was sustained for 20 hours even when the electrode was bent.

7.6 MOF-derived composites

It has been observed that the conductivity of MOFs is improved by hybridization or combination with metal nanoparticles, metal sulfides, and metal oxides in the manufacturing of composite materials made of MOFs for electrocatalysis. The remarkable catalytic, optical, and mechanical characteristics of MOFs and various hybrid materials can be effectively combined in MOF-based composites. The synergistic effect can also trigger new physio-chemical features. In this work, we studied the combination of MOFs with functional constituents for improved electrocatalysis together with reduced graphene oxide (rGO), metal nanoparticles (MNPs), and MXenes, respectively.

Graphene has been employed in many scientific applications owing to its remarkable surface, conductivity, and exceptional stability, and is still reasonably priced. Because of these features, graphene and graphene-based nanomaterials are now widely used in electroanalytical applications. In graphene/MOF composites, higher rates of electron transfer are seen because graphene functions as a conducting bridge in these composites. Based on this concept, firstly, Jayaramulu *et al.* explained the construction of a nanofibrous NGO and a nickel-doped MOF (MOF-74) and showed that the MGO/MOF composite exhibits micro–mesoporous behavior, where the mesopores come from the nickel clusters of MOF associating with the O_2 and N_2 functional groups in the NGO structure, while the micropores come from the pristine MOF.[98] Secondly, with thiourea as a sulfur source, he successfully transforms the NGO/MOF hybrid into a multi-sheet 2D nanocomposite (NGO/Ni_7S_6). In an alkaline solution, the NGO/Ni_7S_6 composite functions as

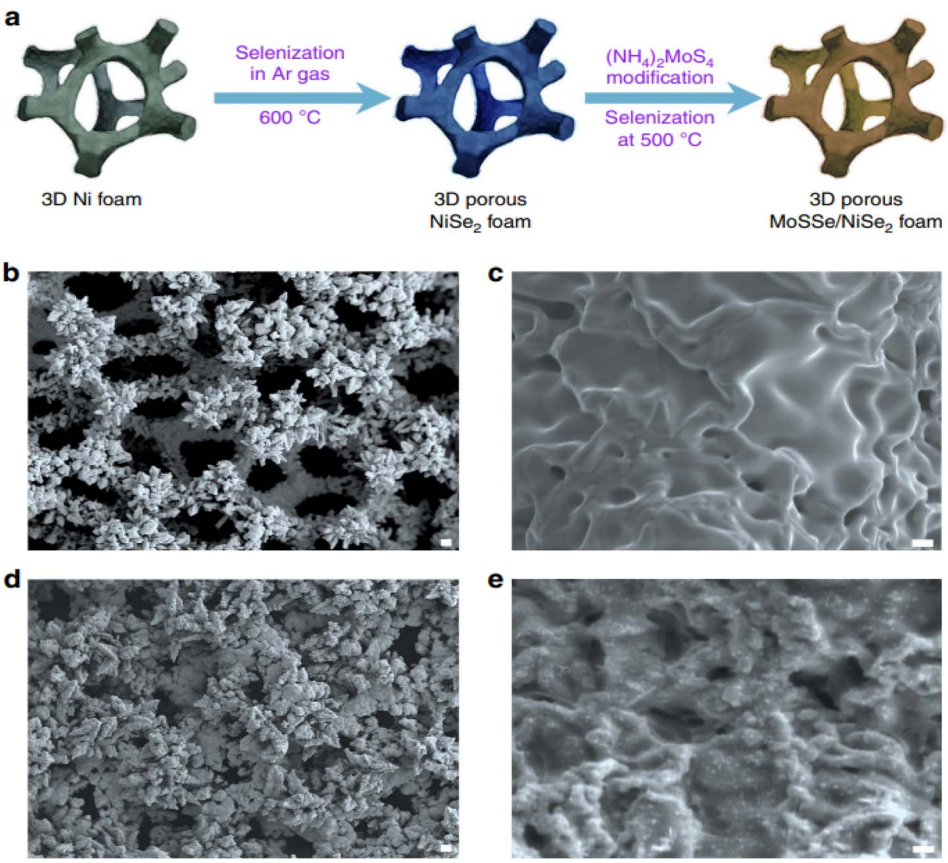

Fig. 13 (a) Procedure for developing $MoS_{2(1-x)}Se_{2x}$ on porous $NiSe_2$ foam. (b and c) SEM images of $NiSe_2$ foam expanded at a temperature of 600 °C from viable nickel foam. (d and e) SEM images of $MoS_{2(1-x)}Se_{2x}$ particles spread over the surface of $NiSe_2$ foam at 500 °C (b and d) scale bar, 50 μm, and (c and e) scale bar, 1 μm. Image is reproduced with permission from ref. 88 under Creative Commons Attribution License CC BY, Copyright © *Nature Communications* 2016.

a perfect bifunctional catalyst for the HER with extreme stability and efficiency. The synergistic effect between Ni_7S_6 and NGO could be liable for the excellent catalytic activity in mass transfer, durability against corrosion over the HER, the quantity of nitrogen, attainable Ni active sites for superior electrical conductivity, and hierarchical porous construction that facilitates rapid mass movement. In another study, Yan *et al.* established the preparation of a AuPd-MnO_x nanocomposite anchored on ZIF-8-rGO bi-supported through wet-chemical techniques[99] as shown in Fig. 14. For the production of hydrogen from FA, the resulting AuPd-MnO_x/ZIF-8-rGO exhibits outstanding catalytic behavior, and at 298 K, the turnover frequency (TOF) achieves its maximum value of 382.1 mol H_2 catalytst per h devoid of any additives. The tuned Pd structure in the AuPd-MnO_x/ZIF-8-rGO hybrids, the reduced dimensions and large diffusion of the AuPd-MnO_x composite, and the durable metal–support interrelation among the AuPd-MnO_x and ZIF-8-rGO bi-support are the motives for this satisfactory catalytic performance of this composite. Through a two-step hydro and solvothermal procedure, Zhu *et al.* loaded MoS_2 onto the Cu-centered MOF and graphene oxide composite to create effective electrocatalysts for the HER.[100] The MoS_2/rGO-MOF composite catalysts have a reduced Tafel slope of 36 mV dec^{-1}, a tiny overpotential of 60 mV, and good electrocatalytic HER activity. The increased surface area resulting from the GO-MOF hybrid's mesoporous structure and the synergistic relation among the GO-MOF matrix and MoS_2 nanosheets were associated with the improvement in catalytic activity. Yun Liu *et al.* successfully used a simple *in situ* space-confined growing approach to create a unique type of MoS_2/3D-NPC composite. High electrocatalytic activity for the HER can be achieved by using MoS_2 nanosheets grown in the pores of highly conductive 3D-NPC. This is because the 3D hierarchical structure can expose the maximum number of active edge sites, provide a strong binding with the conductive carbon host, and facilitate charge transfer during the electrochemical reaction. With a tiny initial overpotential of about 0.16 V, strong cathodic currents, a small Tafel slope of 5 mV per decade, and good stability in acidic media, this 3D architectural composite shows excellent HER activity.[101] Hao Bin Wu *et al.* provided a new method for creating nanostructured MoC_x nano-octahedra as a very effective electrocatalyst for the HER that is aided by MOFs.[102] To achieve uniform formation of metal carbide nanocrystallites without coalescence and excessive growth, this strategy depends on the confined and *in situ* carburization reaction that takes place in a unique MOF-based compound (NENU-5) that consists of a Cu-based MOF (HKUST-1) host and guest Mo-based Keggin POMs residing in pores. These porous MoC_x nano-octahedra, which benefit from the desired nanostructure, show excellent electrocatalytic activity for the HER in basic and acidic solutions with good stability.

Using a "killing three birds with one stone" approach, Li *et al.* developed Fe_3C/Mo_2C-containing N, P, co-doped graphitic carbon from POM@MOF-100 (Fe) (referred to as Fe_3C/Mo_2C@NPGC).[103] One of the best non-noble metal HER catalysts in acidic media reported to date is the Fe_3C/Mo_2C@NPGC catalyst, which exhibits excellent electrocatalytic activity and stability towards the HER with a low onset overpotential of 18 mV (*vs.*RHE), a small Tafel slope of 45.2 mV dec^{-1}, and long-term durability for 10 h. Jia Lu *et al.* used MOFs as functional precursors in a simple pyrolysis process to create multilevel core–shell Au@Zn–Fe–C hybrids.[104] A uniform Zn–Fe-MOFs shell coated on an Au nanoparticle was directly pyrolyzed to develop the nanocomposite hybrids, which demonstrated outstanding electrocatalytic performance for the HER with a low onset overpotential of −0.08 V and a stable current density of 10 mA cm^{-2} at −0.123 V in 0.5 M H_2SO_4. It was

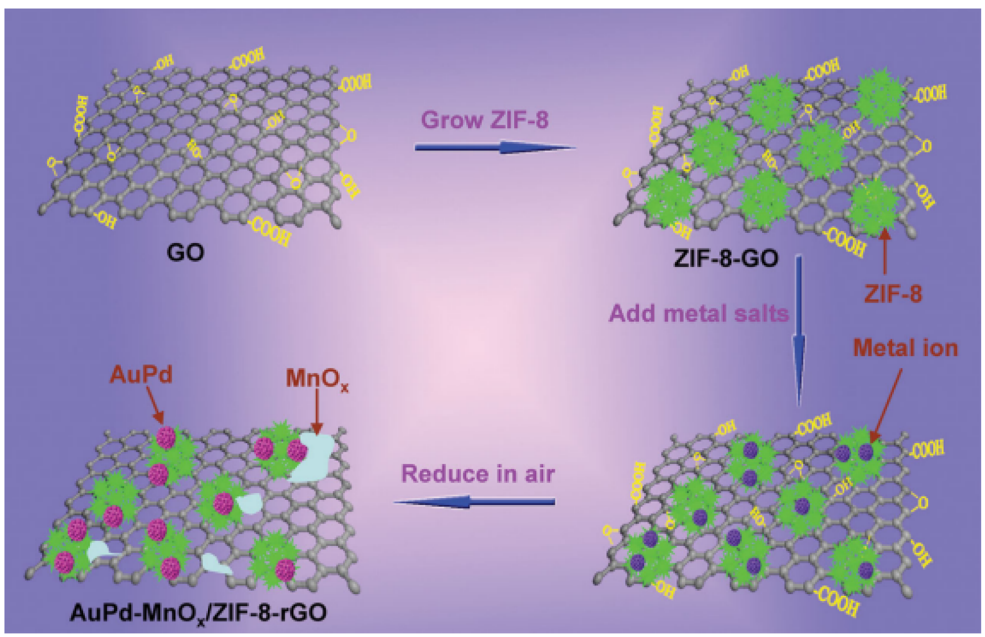

Fig. 14 Diagrammatic representation of the synthesis process of the AuPd-MnO_x/ZIF-8-rGO composite. Image is reproduced with permission from ref. 93 under Creative Commons Attribution License CC BY, Copyright © *Advanced Energy Materials* 2015.

determined that the electrocatalytic activity varied with the loading of the Au nanoparticle cores and the thickness of the metal–carbon shells. This was explained by the conducting shells of Zn–Fe–C for quick electron transport and the creation of active sites for electrocatalytic reactions facilitated by the encapsulated Au nanoparticle.

Pure MOFs' low electroconductivity limits their use in electrochemical domains. To get over this restriction, MXene has become a viable 2D material that can be coupled with MOFs to produce electrocatalysts with excellent surface area, rapid charge transport, and exceptional mechanical stability. Still, the evolution of exceptionally good electrodes is severely constrained in the case where key catalysis mechanisms are poorly understood, and the advancements are still at the synthesis stage. Thus, to expand the applications of electrocatalytic water splitting, a few problems still need to be recognized and resolved. Recently, two-dimensional (2D) MOF nanosheets have been considered ideal electrocatalysts because of their huge number of exposed active metal centers, quick mass and ion transport across their thickness, and porous structure. It is expected that their combination with electrically conductive 2D nanosheets will result in even better electrocatalysis. Regarding this, Zhao and co-workers hybridized two-dimensional cobalt 1,4-benzene dicarboxylate (CoBDC) with $Ti_3C_2T_x$ (the MXene phase) through an *in situ* method.[105] The resultant hybrid material exhibits a Tafel slope of 48.2 mV per decade in 0.1 M KOH and a current density of 10 mA cm^{-2} at a voltage of 1.64 V *vs.* the reversible hydrogen electrode. These outcomes are on par with those attained by the earlier documented transition metal-based catalysts and surpass those achieved by the conventional IrO_2-based catalysts. Very recently, Gothandapani *et al.* synthesized nickel using MXenes (Ni–Ti_3C_2) *via* heating of Ni-MOF at a temperature of 650 °C.[106] The prepared material was examined through XRD, FTIR, FESEM, and BET analysis. Comparable to Ti_3C_2, the resultant Ni–Ti_3C_2 displayed high porosity and a large surface area after calcination. The resulting material was then employed as an electrode for the HER process and examined using several electrochemical techniques, including linear sweep voltammetry (LSV), electrochemical impedance analysis (EIS), and cyclic voltammetry (CV) in an alkaline medium. Due to its surface area and easily obtained active sites, the driven Ni–Ti_3C_2 showed a small Tafel value of 56.15 mV dec^{-1} with a voltage of 181.15 mV, delivering superior electron transport to the Ni–Ti_3C_2 hybrid.

Zong *et al.* proposed MXene-covered MOF-derived cobalt phosphide (Ti_2NT_x@MOF-CoP), a bifunctional catalyst with high activity and low cost.[107] The Ti_2NT_x@MOF-CoP material is developed by phosphating ZIF-67, a substrate that assembles with MXene nanosheets. In a broad pH range, the Ti_2NT_x@-MOF-CoP electrode exhibits modest hydrogen evolution capacity at a current density of 10 mA cm^{-2} and has an inferior overpotential of 112 mV, particularly at pH = 14. They also constructed a dual-electrode for the HER based on the bifunctional activity of Ti_2NT_x@MOF-CoP in alkaline media. Consequently, this study revealed that CoP generated by MOFs offers a large surface area and strong active sites. As a new representative of the MXene, Ti_2NT_x could enhance the heterojunction catalyst stability to expand the active site region.

Incorporating the substrate with ZIF-8 for the HER in an acidic medium, Hao *et al.* reported the production of a $Ti_3C_2T_x$ NS integrated MOF catalyst ($Ti_3C_2T_x$@ZIF-8) with extreme catalytic performance and inexpensiveness.[108] The catalyst has a lower Tafel slope value of 77 mV dec^{-1} and an overpotential of only 507 mV at 20 mA cm^{-2}, which is shown in Fig. 15 (a–d). The active surface area (ECSA) of 122.5 cm^2 is also indicated by CV and chronopotentiometry, which shows that the catalysts are stable over 20 hours with no appreciable variations in the overpotential value.

The combination of CNTs and MOFs results in CNT@MOF hybrids, which have a porous framework that facilitates electrolyte transport through conductive pathways. The addition of CNTs to the CNT@MOF composite, enhanced its conductivity and imparted long-range electron transport capability to the hybrid material. Furthermore, under certain circumstances, by increasing the ratio of surface area to active sites, CNTs help improve the composite's catalytic process, which expands the electrocatalytic activity of MOFs. When electrically conductive CNTs are combined with extremely porous, huge-surface-area MOFs, active CNT@MOF hybrids are produced that function in electrochemical methods. According to Wu *et al.*, cobalt phosphide polyhedral NPs and CNTs were coupled using a MOF templated approach.[109] CoP-CNT hybrids as synthesized exhibit outstanding HER performance because of the synergic catalytic effect among CoP polyhedra and CNTs. In 0.5 M of H_2SO_4, the resulting CoP-CNTs exhibit superior catalytic activity, with an inferior overpotential of ~139 mV at 10 mA cm^{-2}, a tiny onset overpotential of ~64 mV, and a Tafel slope of 52 mV dec^{-1}. The catalysts also exhibit exceptional endurance in acidic solutions.

Transition metal oxides (TMOs) were highly important because of their strong structural stability and superior internal affinity for hydrogen-containing intermediates. Also, by altering the three-dimensional electronic structure of the core metal atom, heterostructure construction could produce an active surface site/relative to the two stages, to enhance electrocatalyst activity. Based on this concept, in recent times, a nanoparticle enriched MOF has been produced by Zhang *et al.*, to synthesize CoFeOx nanoparticles to build a single-layer benzimidazole-based Co-MOF (M-PCBN)[110] With overpotentials of 232, 316, and 348 mV at 10 mA cm^{-2}, M-PCBN showed higher electrocatalytic performance than the massive and pristine MOF, highlighting the importance of including highly catalytically active NPS. A reduced Tafel slope of 32 mV dec^{-1}, and a 60-hour chronoamperometric experiment at 1.48 V *vs.* RHE revealed that M-PCBN exhibited significant stability.

Transition metal sulfides (TMSs) have received attention in electrocatalysts in recent times, due to their excellent redox properties, distinct stoichiometric proportions, high crystallinity, and extremely stable structure. To sustain the reaction intermediates and improve HER capabilities, the extremely electronegative sulfide in TMSs removes electrons from the metal and active sites. Still, several documented TMS-based electrocatalysts have issues such as low conductivity, inferior active sites, and unstable working efficiency. A heterostructure is generally a sensible option for increasing the active area to improve the interfusion effect. Furthermore, by significantly changing the localized ion

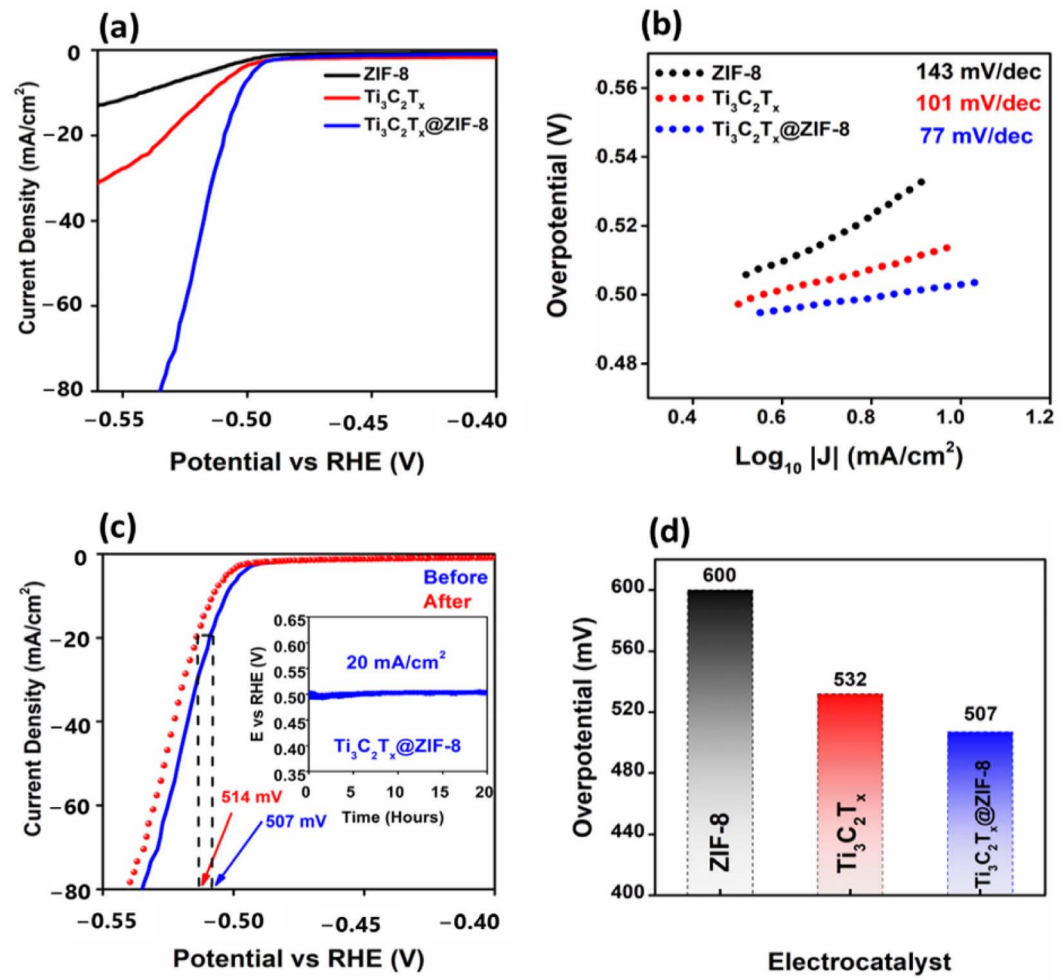

Fig. 15 (a) LSV analysis of ZIF-8, $Ti_3C_2T_x$, and $Ti_3C_2T_x$@ZIF-8 for the HER process. (b) Tafel slope values of ZIF-8, $Ti_3C_2T_x$, and $Ti_3C_2T_x$@ZIF-8. (c) Stability and durability of the $Ti_3C_2T_x$@ZIF-8 electrocatalysts. (d) Histogram for the corresponding overpotential values. Image is reproduced with permission from ref. 97 under Creative Commons Attribution License CC BY, Copyright © *Catalysts* 2023.

and electron transmission behavior, the electron or atomic arrangement at the hetero-unique interface might improve HER catalytic activities. MoS_x on UiO-66-NH_2 was demonstrated by Dai and colleagues *via* a solvothermal approach.[111] At a current density of 10 mA cm^{-2}, the unique construction of the UiO-66-NH_2- stabilized MoS_x-based material showed exceptional HER activity with a Tafel slope of 59 mV dec^{-1}, a potential of 125 mV, and an overpotential of 200 mV. Additionally, it showed exceptional stability in an acidic medium. Its numerous active regions, wide surface area, and rapid electron and proton transport in MOF were the causes of its remarkable HER performance. Qiao and Colleagues recently developed unique 2D hybrid NSs combining MOF-Co-BDC and MoS_2 nanosheets with the electrochemical activity of manufacturing catalysts by a sonication-assisted process.[112] The Co-BDC/MoS_2 electrocatalysts showed significant reaction activity with a Tafel slope of 86 mV dec^{-1} and an overpotential of 248 mV. Additionally, pristine MoS_2 and Co-BDC overpotentials were 349 mV and 529 mV. Furthermore, the nanosheets showed a high degree of dependability for 15 hours at a constant current density of 10 mA cm^{-2}. Co-BDC decorates the semiconducting 2H MoS_2 phase, resulting in a notable phase change to the metallic 1T-MoS_2, which is more suited for the HER process.

Zhen-Feng Huang *et al.* used a simple self-template strategy to develop hollow Co-based bimetallic polyhedra for application in the HER. In this work, solvothermal sulfidation and thermal annealing convert homogeneous bimetallic metal–organic frameworks into hollow bimetallic sulfides. Co_3S_4's HER activity is greatly increased by the combination of the hollow structure and homo-incorporation of a second metal, according to electrochemical experiments and density functional theory calculations. In particular, the Co_3S_4 lattice's homogeneous doping enhances electrical conductivity and maximizes the Gibbs free energy for H* adsorption. Over a broad pH range, hollow $Zn_{0.30}Co_{2.70}S_4$ demonstrates electrocatalytic HER activity better than that in the majority of the reports of noble-metal-free electrocatalysts. In 0.5 M H_2SO_4, 0.1 M phosphate buffer, and 1 M KOH, the overpotentials are 80 mV, 90 mV, and 85 mV at 10 mA cm^{-2}, and 129 mV, 144 mV, and 136 mV at 100 mA cm^{-2} respectively (Table 1).[113]

Table 1 Summary of MOFs and their derivatives as efficient HER electrocatalysts under acid/neutral/alkaline conditions

Electrocatalyst	Electrolyte	Tafel slope (mV dec^{-1})	η @ j (mV@mA^{-2})	Ref.
AB&CTGU-5	0.5 M H_2SO_4	45	44	67
Ni-MOF	0.5 M H_2SO_4	60	350	68
Co-MOF	0.5 M H_2SO_4	121	101	69
2DSP	0.5 M H_2SO_4	80.5	333	70
AB & Co–Cl_4-MOF (3 : 4)	0.5 M H_2SO_4	86	283	71
Py-ZIF	0.5 M H_2SO_4	84	260	73
CuCo@NC	0.5 M H_2SO_4	79	115	74
NiO_x@BCNTs	2 M KOH	119	79	76
Co@Co_3O_4-NC	1 M KOH	77.3	221	77
CoP@NC/CF	1 M KOH	64.8	151.3	78
CoP/NCNHP	0.5 M H_2SO_4	70	310	79
CoP NFs	0.5 M H_2SO_4	49.6	122	80
Ni_2P NS	1 M KOH	63	168	82
Ni_2P/C	0.5 M H_2SO_4	113.2	−94	83
Ni_2P NP	0.5 M H_2SO_4	62	270	84
Co_2Ni_1N	0.5 M H_2SO_4	60.17	102.6	86
Fe–$CoSe_2$@NC	0.5 M H_2SO_4	40	−143	87
$CoSe_2$@DC	0.5 M H_2SO_4	82	−40	88
NiW-CNT/PC/CC	1 M KOH	112.9	45	89
$Ni(OH)_2$/$NiSe_2$/CC	1 M KOH	60	82	90
$NiSe_2$/Ni	0.5 M H_2SO_4	49	143	91
H-$NiSe_2$	0.5 M H_2SO_4	42.6	−107	92
HP-$NiSe_2$	0.5 M H_2SO_4	43	−57	92
$Ni_{0.8}Fe_{0.2}Se_2$/CFC	0.5 M H_2SO_4	43	64	93
SnO_2@$MoSe_2$	0.5 M H_2SO_4	51	174	94
$MoS_{2(1-x)}Se_{2x}$/$NiSe_2$	0.5 M H_2SO_4	42.1	−69	95
$MoSe_2$/$NiSe_2$ NWs	0.5 M H_2SO_4	46.9	249	96
$MoSe_2$	0.5 M H_2SO_4	69.2	305	96
$NiSe_2$	0.5 M H_2SO_4	68.8	345	96
CoS_2 NTA/CC	1 M KOH	88	276	97
Co_3O_4 NWA/CC	1 M KOH	90	350	97
NGO/Ni_7S_6	0.1 M KOH	45.4	161	98
MoS_2/rGO-MOF	0.5 M H_2SO_4	36	60	100
Ni–Ti_3C_2	0.5 M H_2SO_4	56.15	181.1	106
Ti_2NT_x@MOF-CoP	0.5 M H_2SO_4	96.7	129	107
MOF-CoP	0.5 M H_2SO_4	109.4	203	107
ZIF-67	0.5 M H_2SO_4	127.2	256	107
Ti_2NT_x	0.5 M H_2SO_4	172.8	401	107
Ti_2AlN	0.5 M H_2SO_4	245.1	545	107
$Ti_3C_2T_x$@ZIF-8	1 M KOH	77	507	108
CoP-CNTs	0.5 M H_2SO_4	52	139	109
M-PCBN/CC	1 M KOH	32	232	110
Zr-MOF	0.5 M H_2SO_4	59	125	111
Co-BDC/MoS_2	1 M KOH	86	155	112
$Zn_{0.30}Co_{2.70}S_4$	0.5 M H_2SO_4	47.5	80	113
CoP–FeP	0.5 M H_2SO_4	45.1	163	113
MoS_2/3D-NPC	0.5 M H_2SO_4	51	160	101
MoC_x nano-octahedrons	0.5 M H_2SO_4	53	142	102
CoP/GO-400	1 M KOH	135	470	81
Fe_3C/Mo_2C@NPGC	0.5 M H_2SO_4	45.2	18	103
Au@Zn–Fe–C	0.5 M H_2SO_4	130	80	104

8. Summary

In this article, we reviewed the most recent advancements in the development of MOFs and MOF-derived materials as catalysts for water electrolysis. This includes transition metal oxides, sulfides, carbides, and phosphides derived from MOFs. We described and analysed the primary synthesis methods, the current research status of MOF-based materials, the mechanisms of the hydrogen evolution reaction (HER), and the key parameters used to evaluate electrocatalysts. The electrocatalytic performance of pristine MOFs can be enhanced by tailoring their morphology to expose more active sites, developing two-dimensional nanosheet structures, doping with suitable heteroatoms, incorporating conductive materials to

improve electrical conductivity, and modifying their organic ligands. MOF derivatives not only inherit beneficial features of the parent MOFs such as porous structure, high density of active sites, and tuneable pore size, but also exhibit improved chemical stability. Furthermore, the structural design and electronic tuning of MOF materials through various strategies were discussed as approaches to enhance their electrocatalytic activity. Finally, we addressed the importance of ensuring the long-term stability of MOF materials during electrocatalysis in acidic and alkaline environments.

9. Challenges and future perspectives

MOFs offer structural tunability and high surface area; however, their inherent instability in acidic, alkaline, or oxidative environments limits their direct applicability. The metal–ligand bonds in MOFs are prone to degradation, leading to a loss of catalytic activity. While the pyrolysis of MOFs enhances their stability by forming carbonaceous or metallic derivatives, these materials can still suffer from phase transformation or leaching of active sites during prolonged operation. Most pristine MOFs are inherently poor conductors because their organic linkers are generally insulating, which limits their ability to efficiently transfer electrons during electrocatalysis. MOF-derived materials, such as carbonized derivatives, exhibit improved conductivity but often require additional modifications such as doping or hybridization with conductive components to achieve high performance. In MOFs, the density and accessibility of active sites are often limited due to pore blockage or inadequate structural design. During the conversion of MOFs into derived materials, some active sites may be lost due to sintering, aggregation, or incomplete exposure. Although MOFs show high performance under laboratory conditions, their real-world applicability is limited by insufficient stability, high overpotentials, and low current densities at industrial scales.

To address these challenges, researchers are focusing on several strategies. These include developing MOFs with chemically robust linkers, enhancing the stability of MOF-derived materials through protective coatings or encapsulation strategies, and optimizing interfaces in composite materials to withstand operational stress. Additional efforts involve creating conductive MOFs by integrating highly conductive constituents like graphene, carbon nanotubes, or metallic nanoparticles with redox-active or π-conjugated linkers. Engineering MOFs with hierarchical porosity can improve mass transport, while controlled pyrolysis techniques help to preserve or expose active sites in derived materials. Designing composites with well-distributed and accessible catalytic centres is also critical. Addressing these challenges will not only unlock their potential in electrocatalysis but also expand their applicability to other areas like energy storage, gas separation, and sensing.

Data availability

This review article is based solely on previously published data; no new data were generated or collected.

Author contributions

E. S. Sowbakkiyavathi – literature search, data collection, and writing the original draft. Preethi Dhandapani – writing, reviewing & editing. Senthilkumar Ramasamy – reviewing & editing. Ju Hyun Oh & Insik In – reviewing & editing. Seung Jun Lee – funding acquisition, resources, supervision, reviewing & editing. Subramania Angaiah – conceptualization, resources, supervision, validation, funding acquisition, reviewing & editing.

Conflicts of interest

The authors declare no conflict of interest.

Acknowledgements

The authors gratefully acknowledge the financial support from the National Research Foundation of Korea (NRF) through the Brain Pool Program (Grant No. RS-2023-00213746 and RS-2024-00446898) and from the Korea Basic Science Institute (National Research Facilities and Equipment Center), Ministry of Science and ICT (Grant No. RS-2024-00404912).

References

1 N. H. Afgan, D. A. Al Gobaisi, M. G. Carvalho and M. Cumo, Sustainable energy development, *Renew. Sustain. Energy Rev.*, 1998, **2**(3), 235–286.
2 S. Chu, Y. Cui and N. Liu, The path towards sustainable energy, *Nat. Mater.*, 2016, **16**(1), 16–22, DOI: **10.1038/nmat4834**.
3 R. Baños, F. Manzano-Agugliaro, F. G. Montoya, C. Gil, A. Alcayde and J. Gómez, Optimization methods applied to renewable and sustainable energy: A review, *Renew. Sustain. Energy Rev.*, 2011, **15**(4), 1753–1766.
4 S. Chu and A. Majumdar, Opportunities and challenges for a sustainable energy future, *Nature*, 2012, **488**(7411), 294–303.
5 C. Li, H. Zhang, M. Liu, F. F. Lang, J. Pang and X. H. Bu, Recent progress in metal–organic frameworks (MOFs) for electrocatalysis, *Ind. Chem. Mater.*, 2023, **1**(1), 9–38.
6 M. Yue, H. Lambert, E. Pahon, R. Roche, S. Jemei and D. Hissel, Hydrogen energy systems: A critical review of technologies, applications, trends and challenges, *Renew. Sustain. Energy Rev.*, 2021, **146**, 111180, DOI: **10.1016/j.rser.2021.111180**.
7 M. A. Rosen and S. Koohi-Fayegh, The prospects for hydrogen as an energy carrier: an overview of hydrogen energy and hydrogen energy systems, *Energy, Ecol. Environ.*, 2016, **1**(1), 10–29.
8 P. P. Edwards, V. L. Kuznetsov and W. I. F. David, Hydrogen energy, *Philos. Trans. R. Soc. A Math. Phys. Eng. Sci.*, 2007, **365**(1853), 1043–1056.
9 M. Momirlan and T. N. Veziroglu, Current status of hydrogen energy, *Renew. Sustain. Energy Rev.*, 2002, **6**(1–2), 141–179.
10 D. Strmcnik, P. P. Lopes, B. Genorio, V. R. Stamenkovic and N. M. Markovic, Design principles for hydrogen evolution

reaction catalyst materials, *Nano Energy*, 2016, **29**, 29–36, DOI: 10.1016/j.nanoen.2016.04.017.
11 A. Lasia, Mechanism and kinetics of the hydrogen evolution reaction, *Int. J. Hydrogen Energy*, 2019, **44**(36), 19484–19518, DOI: 10.1016/j.ijhydene.2019.05.183.
12 F. Safizadeh, E. Ghali and G. Houlachi, Electrocatalysis developments for hydrogen evolution reaction in alkaline solutions - A Review, *Int. J. Hydrogen Energy*, 2015, **40**(1), 256–274, DOI: 10.1016/j.ijhydene.2014.10.109.
13 O. M. Yaghi, G. Li and H. Li, Selective binding and removal of guests in a microporous metal–organic framework., *Nature*, 1995, **378**, 703–706, DOI: 10.1038/378703a0.
14 H. C. J. Zhou and S. Kitagawa, Metal-Organic Frameworks (MOFs), *Chem. Soc. Rev.*, 2014, **43**(16), 5415–5418.
15 H.-C. Zhou, R. Jeffrey and O. M. Y. Long, Introduction to Metal–Organic Frameworks, *Chem. Rev.*, 2012, **112**(2), 673–674.
16 L. R. Redfern and O. K. Farha, Mechanical properties of metal-organic frameworks, *Chem. Sci.*, 2019, **10**(46), 10666–10679.
17 V. V. Butova, M. A. Soldatov, A. A. Guda, K. A. Lomachenko and C. Lamberti, Metal-organic frameworks: structure, properties, methods of synthesis and characterization, *Russ. Chem. Rev.*, 2016, **85**(3), 280–307.
18 Q. X. Luo, B. W. An, M. Ji and J. Zhang, Hybridization of metal-organic frameworks and task-specific ionic liquids: Fundamentals and challenges, *Mater. Chem. Front.*, 2018, **2**(2), 219–234.
19 D. Chen, C. Han, Q. Sun, J. Ding, Q. Huang, T. T. Li, *et al.*, Bimetallic AgNi nanoparticles anchored onto MOF-derived nitrogen-doped carbon nanostrips for efficient hydrogen evolution, *Green Energy Environ.*, 2023, **8**(1), 258–266, DOI: 10.1016/j.gee.2021.04.003.
20 L. Chai, Z. Hu, X. Wang, Y. Xu, L. Zhang and T. T. Li, Stringing Bimetallic Metal–Organic Framework-Derived Cobalt Phosphide Composite for High-Efficiency Overall Water Splitting, *Adv. Sci.*, 2020, **7**, 1903195, DOI: 10.1002/advs.201903195.
21 N. Danilovic, R. Subbaraman, D. Strmcnik, V. R. Stamenkovic and N. M. Markovic, Electrocatalysis of the HER in acid and alkaline media, *J. Serb. Chem. Soc.*, 2013, **78**(12), 2007–2015.
22 Z. Lv, D. Liu, W. Tian and J. Dang, Designed synthesis of WC-based nanocomposites as low-cost, efficient and stable electrocatalysts for the hydrogen evolution reaction, *CrystEngComm*, 2020, **22**(27), 4580–4590.
23 J. Theerthagiri, S. J. Lee, A. P. Murthy, J. Madhavan and M. Y. Choi, Fundamental aspects and recent advances in transition metal nitrides as electrocatalysts for hydrogen evolution reaction: A review, *Curr. Opin. Solid State Mater. Sci.*, 2020, **24**(1), 100805, DOI: 10.1016/j.cossms.2020.100805.
24 S. Anwar, F. Khan, Y. Zhang and A. Djire, Recent development in electrocatalysts for hydrogen production through water electrolysis, *Int. J. Hydrogen Energy*, 2021, **46**(63), 32284–32317, DOI: 10.1016/j.ijhydene.2021.06.191.
25 H. H. Do, T. H. C. Nguyen, T. V. Nguyen, C. Xia, D. L. T. Nguyen, P. Raizada, *et al.*, Metal-organic-framework based catalyst for hydrogen production: Progress and perspectives, *Int. J. Hydrogen Energy*, 2022, **47**(88), 37552–37568, DOI: 10.1016/j.ijhydene.2022.01.080.
26 N. Zaman, T. Noor and N. Iqbal, Recent advances in the metal-organic framework-based electrocatalysts for the hydrogen evolution reaction in water splitting: a review, *RSC Adv.*, 2021, **11**(36), 21904–21925.
27 A. Udayakumar, P. Dhandapani, S. Ramasamy and S. Angaiah, Layered Double Hydroxide (LDH) – MXene Nanocomposite for Electrocatalytic Water Splitting: Current Status and Perspective, *ES Energy Environ.*, 2023, **20**, 1–18.
28 F. Saraci, V. Quezada-Novoa, P. R. Donnarumma and A. J. Howarth, Rare-earth metal-organic frameworks: From structure to applications, *Chem. Soc. Rev.*, 2020, **49**(22), 7949–7977.
29 D. Yang, V. Bernales, T. Islamoglu, O. K. Farha, J. T. Hupp, C. J. Cramer, *et al.*, Tuning the Surface Chemistry of Metal Organic Framework Nodes: Proton Topology of the Metal-Oxide-Like Zr6 Nodes of UiO-66 and NU-1000, *J. Am. Chem. Soc.*, 2016, **138**(46), 15189–15196.
30 D. Yang, M. Babucci, W. H. Casey and B. C. Gates, The Surface Chemistry of Metal Oxide Clusters: From Metal-Organic Frameworks to Minerals, *ACS Cent. Sci.*, 2020, **6**(9), 1523–1533.
31 Z. Ji, H. Wang, S. Canossa, S. Wuttke and O. M. Yaghi, Pore Chemistry of Metal–Organic Frameworks, *Adv. Funct. Mater.*, 2020, **30**(41), 1–24.
32 Y. Song, X. Li, L. Sun and L. Wang, Metal/metal oxide nanostructures derived from metal-organic frameworks, *RSC Adv.*, 2015, **5**(10), 7267–7279, DOI: 10.1039/C4RA12273A.
33 Y. C. López, H. Viltres, N. K. Gupta, P. Acevedo-Peña, C. Leyva, Y. Ghaffari, *et al.*, Transition metal-based metal–organic frameworks for environmental applications: a review, *Environ. Chem. Lett.*, 2021, **19**, 1295–1334.
34 Y. Zhang, S. Liu, Z. S. Zhao, Z. Wang, R. Zhang, L. Liu, *et al.*, Recent progress in lanthanide metal-organic frameworks and their derivatives in catalytic applications, *Inorg. Chem. Front.*, 2021, **8**(3), 590–619.
35 D. Banerjee, H. Wang, B. J. Deibert and J. Li, *Alkaline Earth Metal-Based Metal – Organic Frameworks: Synthesis, Properties, and Applications*, Chem Met Fram Synth Charact Appl, 2016, ch. 4, pp. 73–103.
36 L. Chen, K. A. San, M. J. Turo, M. Gembicky, S. Fereidouni, M. Kalaj, *et al.*, Tunable Metal Oxide Frameworks via Coordination Assembly of Preyssler-Type Molecular Clusters, *J. Am. Chem. Soc.*, 2019, **141**(51), 20261–20268.
37 P. Z. Moghadam, A. Li, X. W. Liu, R. Bueno-Perez, S. D. Wang, S. B. Wiggin, *et al.*, Targeted classification of metal-organic frameworks in the Cambridge structural database (CSD), *Chem. Sci.*, 2020, **11**(32), 8373–8387.
38 T. K. Kim, K. J. Lee, J. Y. Cheon, J. H. Lee, S. H. Joo and H. R. Moon, Nanoporous metal oxides with tunable and nanocrystalline frameworks via conversion of metal-organic frameworks, *J. Am. Chem. Soc.*, 2013, **135**(24), 8940–8946.

39 H. Deng, C. J. Doonan, H. Furukawa, R. B. Ferreira, J. Towne, C. B. Knobler, *et al.*, Multiple Functional Groups of Varying Ratios in Metal-Organic Frameworks, *Science*, 2010, **327**(5967), 846–851.
40 X. X. Xie, Y. C. Yang, B. H. Dou, Z. F. Li and G. Li, Proton conductive carboxylate-based metal–organic frameworks, *Coord. Chem. Rev.*, 2020, **403**, 213100, DOI: **10.1016/j.ccr.2019.213100**.
41 D. Yang, Y. Chen, Z. Su, X. Zhang, W. Zhang and K. Srinivas, Organic carboxylate-based MOFs and derivatives for electrocatalytic water oxidation, *Coord. Chem. Rev.*, 2021, **428**, 213619, DOI: **10.1016/j.ccr.2020.213619**.
42 X. L. Zhao and W. Y. Sun, The organic ligands with mixed N-/O-donors used in construction of functional metal-organic frameworks, *CrystEngComm*, 2014, **16**(16), 3247–3258.
43 E. D. Bloch, D. Britt, C. Lee, C. J. Doonan, F. J. Uribe-Romo, H. Furukawa, *et al.*, Metal insertion in a microporous metal-organic framework lined with 2,2′-bipyridine, *J. Am. Chem. Soc.*, 2010, **132**(41), 14382–14384.
44 K. J. Gagnon, H. P. Perry and A. Clear, Conventional and Unconventional Metal?Organic Frameworks Based on Phosphonate Ligands: MOFs and UMOFs, *Chem. Rev.*, 2012, **112**(2), 1034–1054.
45 J. D. Lin, J. W. Cheng and S. W. Du, Five d 10 3D Metal–Organic Frameworks Constructed From Aromatic Polycarboxylate Acids and Flexible Imidazole-Based ligands, *Cryst. Growth Des.*, 2008, **8**(9), 2–10.
46 G. X. Liu, K. Zhu, H. M. Xu, S. Nishihara, R. Y. Huang and X. M. Ren, Five 3D metal-organic frameworks constructed from V-shaped polycarboxylate acids and flexible imidazole-based ligands, *CrystEngComm*, 2010, **12**(4), 1175–1185.
47 A. Samokhvalov, Adsorption on Mesoporous Metal-Organic Frameworks in Solution: Aromatic and Heterocyclic Compounds, *Chem.–Eur. J.*, 2015, **21**(47), 16726–16742.
48 R. R. Salunkhe, Y. V. Kaneti and Y. Yamauchi, Metal-Organic Framework-Derived Nanoporous Metal Oxides toward Supercapacitor Applications: Progress and Prospects, *ACS Nano*, 2017, **11**(6), 5293–5308.
49 A. Radwan, H. Jin, D. He and S. Mu, Design Engineering, Synthesis Protocols, and Energy Applications of MOF-Derived Electrocatalysts, *Nano-Micro Lett.*, 2021, **13**, 1–32, DOI: **10.1007/s40820-021-00656-w**.
50 L. T. Glasby, J. L. Cordiner, J. C. Cole and P. Z. Moghadam, Topological Characterization of Metal-Organic Frameworks: A Perspective, *Chem. Mater.*, 2024, **36**, 9013–9030, DOI: **10.1021/acs.chemmater.4c00762**.
51 V. F. Yusuf, N. I. Malek and S. K. Kailasa, Review on Metal-Organic Framework Classification, Synthetic Approaches, and Influencing Factors: Applications in Energy, Drug Delivery, and Wastewater Treatment, *ACS Omega*, 2022, **7**(49), 44507–44531.
52 Y. R. Lee, J. Kim and W. S. Ahn, Synthesis of metal-organic frameworks: A mini review, *Korean J. Chem. Eng.*, 2013, **30**(9), 1667–1680.
53 C. McKinstry, R. J. Cathcart, E. J. Cussen, A. J. Fletcher, S. V. Patwardhan and J. Sefcik, Scalable continuous solvothermal synthesis of metal organic framework (MOF-5) crystals, *J. Chem. Eng.*, 2016, **285**, 718–725, DOI: **10.1016/j.cej.2015.10.023**.
54 K. Kamal, M. A. Bustam, M. Ismail, D. Grekov, A. M. Shariff and P. Pré, Optimization of washing processes in solvothermal synthesis of nickel-based mof-74, *Materials*, 2020, **13**(12), 1–10.
55 D. W. Jung, D. A. Yang, J. Kim, J. Kim and W. S. Ahn, Facile synthesis of MOF-177 by a sonochemical method using 1-methyl-2-pyrrolidinone as a solvent, *Dalton Trans.*, 2010, **39**(11), 2883–2887.
56 Y. R. Lee, M. S. Jang, H. Y. Cho, H. J. Kwon, S. Kim and W. S. Ahn, ZIF-8: A comparison of synthesis methods, *J. Chem. Eng.*, 2015, **271**, 276–280, DOI: **10.1016/j.cej.2015.02.094**.
57 R. Ediati, S. K. Dewi, M. R. Hasan, M. Kahardina, I. K. Murwani and M. Nadjib, Mesoporous HKUST-1 synthesized using solvothermal method, *Rasayan J. Chem.*, 2019, **12**(3), 1653–1659.
58 Y. F. Huang, M. Liu, Y. Q. Wang, Y. Li, J. M. Zhang and S. H. Huo, Hydrothermal synthesis of functionalized magnetic MIL-101 for magnetic enrichment of estrogens in environmental water samples, *RSC Adv.*, 2016, **6**(19), 15362–15369.
59 Y. Li, Y. Liu, W. Gao, L. Zhang, W. Liu, J. Lu, *et al.*, Microwave-assisted synthesis of UIO-66 and its adsorption performance towards dyes, *CrystEngComm*, 2014, **16**(30), 7037–7042.
60 V. A. Soldatov, A. V. Polyakov, V. B. Vera and A. Elena, Erofeeva AAT and, The. MW Synthesis of ZIF-7. The Effect of Solvent on Particle Size and Hydrogen Sorption Properties Vladimir, *Energies*, 2020, **13**(23), 6309.
61 V. I. Isaeva, V. I. Isaeva, B. R. Saifutdinov, V. V. Chernyshev, V. V. Chernyshev, V. V. Vergun, *et al.*, Impact of the preparation procedure on the performance of the microporous HKUST-1 metal-organic framework in the liquid-phase separation of aromatic compounds, *Molecules*, 2020, **25**(11), 1–21.
62 Z. Cao, R. Momen, S. Tao, D. Xiong, Z. Song, X. Xiao, *et al.*, Metal–Organic Framework Materials for Electrochemical Supercapacitors, *Nano-Micro Lett.*, 2022, **14**, 1–33, DOI: **10.1007/s40820-022-00910-9**.
63 V. Sharma, Metal-Organic Frameworks Driven Electrocatalytic and Photocatalytic Hydrogen Production: A Mini-Review, *Biointerface Res. Appl. Chem.*, 2023, **13**(3), 1–11.
64 Y. Fu, H. Wang, N. Li, L. Mao, X. Wang, Y. Fu, *et al.*, Pt inclusion effect on Ni-ABDC-derived PtNi-carbon nanomaterials for hydrogen evolution, *Chin. Chem. Lett.*, 2025, 110890, DOI: **10.1016/j.cclet.2025.110890**.
65 A. Mahmood, W. Guo, H. Tabassum and R. Zou, Metal-Organic Framework-Based Nanomaterials for Electrocatalysis, *Adv. Energy Mater.*, 2016, **6**, 1–26, DOI: **10.1002/aenm.201600423**.
66 M. S. S. Danish, Exploring metal oxides for the hydrogen evolution reaction (HER) in the field of nanotechnology, *RSC Sustain.*, 2023, **1**(9), 2180–2196.

67 Y. P. Wu, W. Zhou, J. Zhao, W. W. Dong, Y. Q. Lan, D. S. Li, *et al.*, Surfactant-Assisted Phase-Selective Synthesis of New Cobalt MOFs and Their Efficient Electrocatalytic Hydrogen Evolution Reaction, *Angew. Chem., Int. Ed.*, 2017, **56**(42), 13001–13005.

68 V. Khrizanforova, R. Shekurov, V. Miluykov, M. Khrizanforov, V. Bon, S. Kaskel, *et al.*, 3D Ni and Co redox-active metal-organic frameworks based on ferrocenyl diphosphinate and 4,4′-bipyridine ligands as efficient electrocatalysts for the hydrogen evolution reaction, *Dalton Trans.*, 2020, **49**(9), 2794–2802.

69 Y. C. Zhou, W. W. Dong, M. Y. Jiang, Y. P. Wu, D. S. Li, Z. F. Tian, *et al.*, A new 3D 8-fold interpenetrating 66-dia topological Co-MOF: Syntheses, crystal structure, magnetic properties and electrocatalytic hydrogen evolution reaction, *J. Solid State Chem.*, 2019, **279**, 120929, DOI: **10.1016/j.jssc.2019.120929**.

70 R. Dong, M. Pfeffermann, H. Liang, Z. Zheng, X. Zhu, J. Zhang, *et al.*, Large-Area, Free-Standing, Two-Dimensional Supramolecular Polymer Single-Layer Sheets for Highly Efficient Electrocatalytic Hydrogen Evolution, *Angew. Chem., Int. Ed.*, 2015, **54**(41), 12058–12063.

71 Y. S. Li, J. W. Yi, J. H. Wei, Y. P. Wu, B. Li and S. Liu, Three 2D polyhalogenated Co(II)-based MOFs: Syntheses, crystal structure and electrocatalytic hydrogen evolution reaction, *J. Solid State Chem.*, 2020, **281**, 1–20, DOI: **10.1016/j.jssc.2019.121052**.

72 T. Wang, Q. Zhou, X. Wang, J. Zheng and X. Li, MOF-derived surface modified Ni nanoparticles as an efficient catalyst for the hydrogen evolution reaction, *J. Mater. Chem. A*, 2015, **3**(32), 16435–16439.

73 W. Zhao, G. Wan, C. Peng, H. Sheng, J. Wen and H. Chen, Key Single-Atom Electrocatalysis in Metal—Organic Framework (MOF)-Derived Bifunctional Catalysts, *ChemSusChem*, 2018, **11**(19), 3473–3479.

74 M. Kuang, Q. Wang, P. Han and G. Zheng, Cu, Co-Embedded N-Enriched Mesoporous Carbon for Efficient Oxygen Reduction and Hydrogen Evolution Reactions, *Adv. Energy Mater.*, 2017, **7**(17), 1–8.

75 N. Mahmood, Y. Yao, J. W. Zhang, L. Pan, X. Zhang and J. J. Zou, Electrocatalysts for Hydrogen Evolution in Alkaline Electrolytes: Mechanisms, Challenges, and Prospective Solutions, *Adv. Sci.*, 2018, **5**, 1–23, DOI: **10.1002/advs.201700464**.

76 J. Wang, S. Mao, Z. Liu, Z. Wei, H. Wang, Y. Chen, *et al.*, Dominating Role of Ni0 on the Interface of Ni/NiO for Enhanced Hydrogen Evolution Reaction, *ACS Appl. Mater. Interfaces*, 2017, **9**(8), 7139–7147.

77 C. Bai, S. Wei, D. Deng, X. Lin, M. Zheng and Q. Dong, A nitrogen-doped nano carbon dodecahedron with Co@Co3O4 implants as a bi-functional electrocatalyst for efficient overall water splitting, *J. Mater. Chem. A*, 2017, **5**(20), 9533–9536, DOI: **10.1039/C7TA01708A**.

78 Y. Wang, S. Li, Y. Chen, X. Shi, C. Wang and L. Guo, 3D hierarchical MOF-derived CoP@N-doped carbon composite foam for efficient hydrogen evolution reaction, *Appl. Surf. Sci.*, 2020, **505**, 144503, DOI: **10.1016/j.apsusc.2019.144503**.

79 Y. Pan, K. Sun, S. Liu, X. Cao, K. Wu, W. C. Cheong, *et al.*, Core-Shell ZIF-8@ZIF-67-Derived CoP Nanoparticle-Embedded N-Doped Carbon Nanotube Hollow Polyhedron for Efficient Overall Water Splitting, *J. Am. Chem. Soc.*, 2018, **140**(7), 2610–2618.

80 L. Ji, J. Wang, X. Teng, T. J. Meyer and Z. Chen, CoP Nanoframes as Bifunctional Electrocatalysts for Efficient Overall Water Splitting, *ACS Catal.*, 2020, **10**(1), 412–419.

81 L. Jiao, Y. X. Zhou and H. L. Jiang, Metal-organic framework-based CoP/reduced graphene oxide: High-performance bifunctional electrocatalyst for overall water splitting, *Chem. Sci.*, 2016, **7**(3), 1690–1695, DOI: **10.1039/C5SC04425A**.

82 Q. Wang, Z. Liu, H. Zhao, H. Huang, H. Jiao and Y. Du, MOF-derived porous Ni2P nanosheets as novel bifunctional electrocatalysts for the hydrogen and oxygen evolution reactions, *J. Mater. Chem. A*, 2018, **6**(38), 18720–18727.

83 S. He, S. He, X. Bo, Q. Wang, F. Zhan, Q. Wang, *et al.*, Porous Ni2P/C microrods derived from microwave-prepared MOF-74-Ni and its electrocatalysis for hydrogen evolution reaction, *Mater. Lett.*, 2018, **231**, 94–97, DOI: **10.1016/j.matlet.2018.08.033**.

84 T. Tian, L. Ai and J. Jiang, Metal-organic framework-derived nickel phosphides as efficient electrocatalysts toward sustainable hydrogen generation from water splitting, *RSC Adv.*, 2015, **5**(14), 10290–10295, DOI: **10.1039/C4RA15680C**.

85 F. Tian, D. F. Hou, W. Zhang and X. Q. Qiao, Synthesis of Ni2P/Ni12P5 bi-phase nanocomposite for efficient catalytic reduction of 4-nitrophenol based on the unique n-n heterojunction effects, *Dalton Trans.*, 2017, **46**(41), 14107–14113, DOI: **10.1039/C7DT02375H**.

86 X. Feng, H. Wang, X. Bo and L. Guo, Bimetal-Organic Framework-Derived Porous Rodlike Cobalt/Nickel Nitride for All-pH Value Electrochemical Hydrogen Evolution, *ACS Appl. Mater. Interfaces*, 2019, **11**(8), 8018–8024.

87 X. Wu, S. Han, D. He, C. Yu, C. Lei, W. Liu, *et al.*, Metal Organic Framework Derived Fe-Doped CoSe2 Incorporated in Nitrogen-Doped Carbon Hybrid for Efficient Hydrogen Evolution, *ACS Sustain. Chem. Eng.*, 2018, **6**(7), 8672–8678.

88 W. Zhou, J. Lu, K. Zhou, L. Yang, Y. Ke, Z. Tang, *et al.*, CoSe2 nanoparticles embedded defective carbon nanotubes derived from MOFs as efficient electrocatalyst for hydrogen evolution reaction, *Nano Energy*, 2016, **28**, 143–150, DOI: **10.1016/j.nanoen.2016.08.040**.

89 X. Wang, Z. Qin, J. Qian and L. Chen, Self-Supporting Hierarchical Carbon Network Loaded with NiW Nanoparticles for Efficient Hydrogen Evolution, *Small*, 2024, **20**, 1–8, DOI: **10.1002/smll.202405063**.

90 C. Liu, Q. Chen, Q. Hao, X. Zheng, S. Li, D. Jia, *et al.*, Ni(OH) 2/NiSe 2 hybrid nanosheet arrays for enhanced alkaline hydrogen evolution reaction, *Int. J. Hydrogen Energy*, 2019, **44**(10), 4832–4838, DOI: **10.1016/j.ijhydene.2018.12.194**.

91 H. Zhou, Y. Wang, R. He, F. Yu, J. Sun, F. Wang, *et al.*, One-step synthesis of self-supported porous NiSe2/Ni hybrid foam: An efficient 3D electrode for hydrogen evolution reaction, *Nano Energy*, 2016, **20**, 29–36.

92 H. Zhou, F. Yu, Y. Liu, J. Sun, Z. Zhu, R. He, *et al.*, Outstanding hydrogen evolution reaction catalyzed by porous nickel diselenide electrocatalysts, *Energy Environ. Sci.*, 2017, **10**(6), 1487–1492, DOI: 10.1039/c7ee00802c.

93 T. Wang, D. Gao, W. Xiao, P. Xi, D. Xue and J. Wang, Transition-metal-doped NiSe2 nanosheets towards efficient hydrogen evolution reactions, *Nano Res.*, 2018, **11**(11), 6051–6061.

94 Y. Huang, Y. E. Miao, J. Fu, S. Mo, C. Wei and T. Liu, Perpendicularly oriented few-layer MoSe2 on SnO2 nanotubes for efficient hydrogen evolution reaction, *J. Mater. Chem. A*, 2015, **3**(31), 16263–16271.

95 H. Zhou, F. Yu, Y. Huang, J. Sun, Z. Zhu, R. J. Nielsen, *et al.*, Efficient hydrogen evolution by ternary molybdenum sulfoselenide particles on self-standing porous nickel diselenide foam, *Nat. Commun.*, 2016, **7**, 1–7, DOI: 10.1038/ncomms12765.

96 L. Zhang, T. Wang, L. Sun, Y. Sun, T. Hu, K. Xu, *et al.*, Hydrothermal synthesis of 3D hierarchical MoSe2/NiSe2 composite nanowires on carbon fiber paper and their enhanced electrocatalytic activity for the hydrogen evolution reaction, *J. Mater. Chem. A*, 2017, **5**(37), 19752–19759.

97 C. Guan, X. Liu, A. M. Elshahawy, H. Zhang, H. Wu, S. J. Pennycook, *et al.*, Metal-organic framework derived hollow CoS2 nanotube arrays: An efficient bifunctional electrocatalyst for overall water splitting, *Nanoscale Horiz.*, 2017, **2**(6), 342–348, DOI: 10.1039/c7nh00079k.

98 K. Jayaramulu, J. Masa, O. Tomanec, D. Peeters, V. Ranc, A. Schneemann, *et al.*, Nanoporous Nitrogen-Doped Graphene Oxide/Nickel Sulfide Composite Sheets Derived from a Metal-Organic Framework as an Efficient Electrocatalyst for Hydrogen and Oxygen Evolution, *Adv. Funct. Mater.*, 2017, **27**(33), 1–10.

99 J. M. Yan, Z. L. Wang, L. Gu, S. J. Li, H. L. Wang, W. T. Zheng, *et al.*, AuPd-MnOx/MOF-graphene: An efficient catalyst for hydrogen production from formic acid at room temperature, *Adv. Energy Mater.*, 2015, **5**(10), 10–15.

100 C. Zhu, K. Wang, T. Lei, T. Xiao and L. Liu, Facile synthesis of MoS2/rGO-MOF hybrid material as highly efficient catalyst for hydrogen evolution, *Mater. Lett.*, 2018, **216**, 243–247, DOI: 10.1016/j.matlet.2018.01.123.

101 Y. Liu, X. Zhou, T. Ding, C. Wang and Q. Yang, 3D architecture constructed via the confined growth of MoS2 nanosheets in nanoporous carbon derived from metal-organic frameworks for efficient hydrogen production, *Nanoscale*, 2015, **7**(43), 18004–18009.

102 H. B. Wu, B. Y. Xia, L. Yu, X. Y. Yu and X. W. Lou, Porous molybdenum carbide nano-octahedrons synthesized via confined carburization in metal-organic frameworks for efficient hydrogen production, *Nat. Commun.*, 2015, **6**, 1–8.

103 J. S. Li, Y. J. Tang, C. H. Liu, S. L. Li, R. H. Li, L. Z. Dong, *et al.*, Polyoxometalate-based metal-organic framework-derived hybrid electrocatalysts for highly efficient hydrogen evolution reaction, *J. Mater. Chem. A*, 2016, **4**(4), 1202–1207, DOI: 10.1039/C5TA09743F.

104 J. Lu, W. Zhou, L. Wang, J. Jia, Y. Ke, L. Yang, *et al.*, Core-Shell Nanocomposites Based on Gold Nanoparticle@Zinc-Iron-Embedded Porous Carbons Derived from Metal-Organic Frameworks as Efficient Dual Catalysts for Oxygen Reduction and Hydrogen Evolution Reactions, *ACS Catal.*, 2016, **6**(2), 1045–1053.

105 L. Zhao, B. Dong, S. Li, L. Zhou, L. Lai, Z. Wang, *et al.*, Interdiffusion Reaction-Assisted Hybridization of Two-Dimensional Metal-Organic Frameworks and Ti3C2Tx Nanosheets for Electrocatalytic Oxygen Evolution, *ACS Nano*, 2017, **11**(6), 5800–5807.

106 K. Gothandapani, G. Tamil Selvi, R. Sofia Jennifer, V. Velmurugan, S. Pandiaraj, M. Muthuramamoorthy, S. Pitchaimuthu, V. Raghavan, A. Christina Josephine Malathi, A. Alodhayb and A. N. Grace, Ni-Ti C MXene composite derived from Ni-metal organic framework for electrochemical hydrogen evolution reaction in acidic and alkaline medium, *Int. J. Hydrogen Energy*, 2023, **52**, 1–17, DOI: 10.1016/j.ijhydene.2023.10.022.

107 H. Zong, R. Qi, K. Yu and Z. Zhu, Ultrathin Ti2NTx MXene-wrapped MOF-derived CoP frameworks towards hydrogen evolution and water oxidation, *Electrochim. Acta*, 2021, **393**, 1–10, DOI: 10.1016/j.electacta.2021.139068.

108 L. P. Hao, A. Hanan, R. Walvekar, M. Khalid, F. Bibi, W. Y. Wong, *et al.*, Synergistic Integration of MXene and Metal-Organic Frameworks for Enhanced Electrocatalytic Hydrogen Evolution in an Alkaline Environment, *Catalysts*, 2023, **13**(5), 1–13.

109 C. Wu, Y. Yang, D. Dong, Y. Zhang and J. Li, In Situ Coupling of CoP Polyhedrons and Carbon Nanotubes as Highly Efficient Hydrogen Evolution Reaction Electrocatalyst, *Small*, 2017, **13**(15), 1–9.

110 W. Zhang, Y. Wang, H. Zheng, R. Li, Y. Tang, B. Li, *et al.*, Embedding Ultrafine Metal Oxide Nanoparticles in Monolayered Metal-Organic Framework Nanosheets Enables Efficient Electrocatalytic Oxygen Evolution, *ACS Nano*, 2020, **14**(2), 1971–1981.

111 X. Dai, M. Liu, Z. Li, A. Jin, Y. Ma, X. Huang, *et al.*, Molybdenum Polysulfide Anchored on Porous Zr-Metal Organic Framework to Enhance the Performance of Hydrogen Evolution Reaction, *J. Phys. Chem. C*, 2016, **120**(23), 12539–12548.

112 D. Zhu, J. Liu, Y. Zhao, Y. Zheng and S. Z. Qiao, Engineering 2D Metal–Organic Framework/MoS 2 Interface for Enhanced Alkaline Hydrogen Evolution, *Small*, 2019, **15**(14), 1–8.

113 Z. F. Huang, J. Song, K. Li, M. Tahir, Y. T. Wang, L. Pan, *et al.*, Hollow Cobalt-Based Bimetallic Sulfide Polyhedra for Efficient All-pH-Value Electrochemical and Photocatalytic Hydrogen Evolution, *J. Am. Chem. Soc.*, 2016, **138**(4), 1359–1365.